Social Neuroscience

ISSN: 1747-0919 (Print) 1747-0927 (Online) Journal homepage: https://www.tandfonline.com/loi/psns20

Spatio-temporal dynamics of the mirror neuron system during social intentions

Stephanie Cacioppo, Mylene Bolmont & George Monteleone

To cite this article: Stephanie Cacioppo, Mylene Bolmont & George Monteleone (2018) Spatio-temporal dynamics of the mirror neuron system during social intentions, Social Neuroscience, 13:6, 718-738, DOI: 10.1080/17470919.2017.1394911

To link to this article: https://doi.org/10.1080/17470919.2017.1394911

Accepted author version posted online: 19 Oct 2017.
Published online: 27 Oct 2017.

SOCIAL NEUROSCIENCE
2018, VOL. 13, NO. 6, 718–738
https://doi.org/10.1080/17470919.2017.1394911

Routledge
Taylor & Francis Group

ARTICLE

Spatio-temporal dynamics of the mirror neuron system during social intentions

Stephanie Cacioppo[a,b], Mylene Bolmont[c] and George Monteleone[b]

[a]Department of Psychiatry and Behavioural Neuroscience, University of Chicago Pritzker School of Medicine, Chicago, IL, USA; [b]High-Performance Electrical Neuroimaging Laboratory, Center for Cognitive and Social Neuroscience, University of Chicago, Chicago, IL, USA; [c]Department of Psychology, University of Geneva, Geneva, Switzerland

ABSTRACT

Previous research has shown that specific goals and intentions influence a person's allocation of social attention. From a neural viewpoint, a growing body of evidence suggests that the inferior fronto-parietal network, including the mirror neuron system, plays a role in the planning and the understanding of motor intentions. However, it is unclear whether and when the mirror neuron system plays a role in social intentions. Combining a behavioral task with electrical neuroimaging in 22 healthy male participants, the current study investigates whether the temporal brain dynamic of the mirror neuron system differs during two types of social intentions i.e., lust vs. romantic intentions. Our results showed that 62% of the stimuli evoking lustful intentions also evoked romantic intentions, and both intentions were sustained by similar activations of the inferior frontal gyrus and the inferior parietal lobule/angular gyrus for the first 432 ms after stimulus onset. Intentions to not love or not lust, on the other hand, were characterized by earlier differential activations of the inferior fronto-parietal network i.e., as early as 244 ms after stimulus onset. These results suggest that the mirror neuron system may not only code for the motor correlates of intentions, but also for the social meaning of intentions and its valence at both early/automatic and later/more elaborative stages of information processing.

ARTICLE HISTORY
Received 6 April 2017
Revised 13 September 2017
Published online 27 October 2017

KEYWORDS
Electrical neuroimaging; mirror neuron system; brain dynamics; social intentions; love; desire; and interpersonal attraction

Introduction

When you are online dating, looking at photo portraits of potential mates, how do you evaluate whether she/he has any intentions to be in a romantic, lasting relationship with you? This question is bidirectional. What intention goes through your mind when you decide to swipe right, for instance, and want to go on a date with a person? That is a question 25 million Tinder users (as of 2016) may wonder when they are on this online dating application. While Tinder does not differentiate a "romantic" swipe from a "lust/one night stand" swipe, our prior work suggest that these two social intentions can be differentiated as they are sustained by different visual attentional mechanisms (Bolmont, Cacioppo, & Cacioppo, 2014; S. Cacioppo, 2016; S. Cacioppo & Cacioppo, 2013; S. Cacioppo et al., 2013a). This is in accord with a growing body of studies showing that specific goals and intentions influence a person's allocation of social attention (Argyle & Cook, 1976; Baron-Cohen, 1995; Emery, 2000; Jones, Main, DeBruine, Little, & Welling, 2010; Rupp & Wallen, 2007), and that intentions are functionally coupled with selective visual processing before action (e.g., Land & Lee, 1994; Land, Mennie, & Rusted, 1999).

From a neural viewpoint, it has been suggested that the inferior fronto-parietal network, including the mirror neuron system, plays a facilitating role in the processing and planning of motor intentions (Ortigue, Sinigaglia, Rizzolatti, & Grafton, 2010b; Ortigue, Thompson, Parasuraman, & Grafton, 2009; Rizzolatti, Fadiga, Gallese, & Fogassi, 1996; Rizzolatti & Sinigaglia, 2007, 2008, 2010; S. Cacioppo, Juan, & Monteleone, 2017). Indeed, while the early studies on mirror neurons in monkeys (Gallese, Fadiga, Fogassi, & Rizzolatti, 1996; Rizzolatti et al., 1996) described a mechanism allowing the observer to only understand *what* an individual was doing in a given moment (e.g., touching, grasping), more recent data indicate that the mirror neuron system might also account for the capacity to understand *why* the agent was doing it, that is the agent's *motor intention* (Rizzolatti & Sinigaglia, 2007, 2008, 2010; Ortigue et al., 2010b; S. Cacioppo, Juan & Monteleone, 2017). Fogassi, Ferrari, Gesierich, Rozzi, and Chersi et al. (2005), for instance, showed that, in the inferior parietal lobule (IPL) of the monkey, the majority of motor neurons discharge during a motor act (e.g., grasping) only if this act is embedded in a specific chain of motor intentional acts (e.g., grasping-for-eating). Most interestingly,

CONTACT Stephanie Cacioppo scacioppo@bsd.uchicago.edu University of Chicago, 940 E. 57th, Chicago, IL 60637, USA

many of these "action-constrained" motor neurons have mirror properties firing in relation to the observation of a motor act provided that this act is part of a specific action. By virtue of these "action-constrained" mirror neurons and their motor connections, the observation of the initial motor act of an action evokes in the observer's brain an internal motor copy of the action that the agent is going to perform, and this enables her/him to understand the intention underlying the observed motor act. Brain imaging data indicate that the mirror mechanism plays a role in intention understanding in humans, as well (Hamilton & Grafton, 2008; Iacoboni et al., 2005; Juan et al., 2013; Ortigue et al., 2009, 2010b; S. Cacioppo, Juan & Monteleone, 2017). Moreover, by using electromyogram (EMG), it has been shown that the observation of the initial motor act (e.g., grasping) of an intentional action (grasping a piece of food to eat it) evokes in human observers a motor copy of the action the agent is going to perform. This motor copy allows the observer to grasp the agent's intention, without bringing into play specialized inferential processes of mentalistic rationalization (S. Cacioppo et al., 2014a; Cattaneo et al., 2007). A similar brain network is recruited during the preparation of a motor intentional act (Cunnington, Windischberger, Robinson, & Moser, 2006; Majdandžić et al., 2007; Ramnani & Miall, 2004; Toni, Thoenissen, & Zilles, 2001). During the preparation for intentional action, prior to initiation, higher motor areas, including dorsal premotor cortex (DLPMC) and ventral premotor cortex (VPMC), the superior parietal cortex, and the pre-supplementary motor area (pre-SMA) are activated in addition of the posterior superior temporal sulcus (pSTS), posterior middle temporal gyrus (pMTG), the inferior frontal gyrus and the inferior parietal lobule, which are specifically activated during the observation of intentional actions (Cunnington et al., 2006; Juan et al., 2013 for review; Lewis, 2006; Toni et al., 2001). When intentions are embedded in a more social context (e.g., intention to help; Wang et al., 2016; Yu, Cai, Shen, Gao, & Zhou, 2016), brain areas involved in social interaction are also recruited (Grafton, 2009; Juan et al., 2013 for reviews). These "social" brain areas include the insula, ventro-medial prefrontal cortex (vMPFC), precuneate cortex, posterior cingulate cortex, amygdala, the superior temporal sulcus (STS), and the region that goes beyond the fundus and the banks of STS; the superior temporal gyrus (STG), the middle temporal gyrus (MTG), and the part of the angular gyrus that is near the ascending limb of STS (Allison, Puce, & McCarthy, 2000; Ortigue et al., 2009; Yu et al., 2016).

From a timing perspective, methods using millisecond temporal resolution, such as high-density EEG and/or magneto-encephalography (MEG) are perfectly suited to investigate the temporal brain dynamics of intention understanding and recent methodological improvement in brain state identification, head models, and more reliable cortical source localization techniques hold significant promise to suggest potential underlying spatial dynamics. However, to date, the temporal dynamics of intention has been limited to the study of motor intentions and/or intention decoding of actions performed by others (e.g., Friston & Frith, 2015; Honaga et al., 2010; Ortigue et al., 2009, 2010b; Van der Cruyssen, Van Duynslaeger, Cortoos, & Van Overwalle, 2009; Van Duynslaeger, Van Overwalle, & Verstraeten, 2007; Vistoli et al., 2015). For example, Van der Cruyssen et al. (2009) tried to specify the temporal dynamics of decoding intentions of others by performing an event-related potential (ERP) study where participants had to decode intentions based on the reading of the last word of sentences describing the behaviour of an agent, and from which a specific intention could be inferred. Because this task was driven by verbal cues, it remains unclear whether these findings could generalize to the decoding of intentions in social settings or to the participant's own intentions. Although a number of studies have investigated the neural bases of a broad variety of intentions, nothing is known about the *temporal dynamics* of these brain areas during social intentions, like romantic intentions or lustful intentions.

The aim of the present study is to describe the temporal sequence of brain activation that sustain one's romantic or lustful intention toward someone. The digital revolution and the development of the internet, recent advances in technologies, and the growing number of online dating sites make this question not only sensible to address, but ecologically valid. Based on psychological theories that suggest overlap between the construct of love and the construct of lust, such as the awareness of wanting (or wishing) to attain a potentially pleasurable goal that is currently unattainable or uncertain (Hatfield & Rapson, 2005, 2009; Regan, 1998), we hypothesized that the intentions to lust and intentions to romantically love show considerable overlap and share common psychobiological processes. In addition, based on clinical evidence and neuroimaging studies showing differences between lust and love with love being a more abstract representation of the pleasant sensorimotor experiences that characterize lust (Bolmont et al., 2014; S. Cacioppo, 2016, 2017a; S. Cacioppo, Bianchi-Demicheli, Hatfield, & Rapson, 2012b; S. Cacioppo & Hatfield, 2013; Hatfield & Rapson, 2005, 2009; Regan, 1998, 1999; Regan & Berscheid, 1999), we also hypothesized that intentions to lust would be processed differently (and faster) than the intentions to love. The alternative hypothesis is that intentions to love or lust are characterized by similar brain dynamics.

To test these hypotheses, we used one of our standard behavioral social intention paradigms (Bolmont et al., 2014; S. Cacioppo et al., 2013a), in which participants are asked to view photographs of attractive strangers and decide rapidly whether they have the intention to be in a lustful relationship or a romantic relationship with each depicted individual, while brain activity was recorded with high-density electroencephalogram. The paradigm has been tested successfully in different countries (e.g., Bolmont et al., 2014; S. Cacioppo, 2016; S. Cacioppo et al., 2013a).

As a method of analysis, we used high-density electrical neuroimaging, which combined a cluster-analysis of brain topography (a technique originally elaborated by Lehmann, 1987, and recently modified by S. Cacioppo & Cacioppo, 2015; S. Cacioppo, 2017b) with inverse solutions. This method has the advantage of providing high temporal and a relatively high spatial resolution about stimulus information processing by unravelling the temporal sequence of the periods of brain topographies (brain microstates) that are stable after a stimulus onset and the spatial location of the brain generators of these brain topographies. This technique has already been proven to be a reliable research tool during the past decade (e.g., S. Cacioppo, 2017b; S. Cacioppo & Cacioppo, 2015; S. Cacioppo et al., 2013b; S. Cacioppo, Weiss, Runesha, & Cacioppo, 2014b, 2016; Murray, Brunet, & Michel, 2008; Ortigue & Bianchi-Demicheli, 2008; Ortigue et al., 2004). The use of this multidimensional approach in the present study provides critical insights into the spatiotemporal brain dynamics during social intentions to love and intentions to lust.

Although both love and lust sit on top of the main emotional experiences that are investigated in couples' therapy, there are still debates about the brain dynamics and origin of these two subjective experiences (S. Cacioppo, Bianchi-Demicheli, Frum, Pfaus, & Lewis, 2012a for review; Hatfield & Rapson, 2009; Regan, 1998, 1999; Regan & Berscheid, 1999). The specificity of love and lust is a critical question as these two phenomena may occur in concert (S. Cacioppo & Cacioppo, 2013), making it often difficult to dissociate what phenomenon modulates the source of a couple's difficulties. Decades of investigations on love and sexual attitudes have shed light on potential confounding factors between love and lust (Diamond, 2004, Hatfield & Rapson, 2005; Hendrick & Hendrick, 1987, 1995; Tennov, 1998). Both parallels (e.g., Hendrick & Hendrick, 1987, 1995) and differences between love attitudes and sexual attitudes (S. Cacioppo & Hatfield, 2013; S. Cacioppo et al., 2012b) have been delineated. Love is defined here as "a state of intense longing for union with another" (Ortigue, Bianchi-Demicheli, Patel, Frum, & Lewis, 2010a; S. Cacioppo & Hatfield, 2013), but it is clear that it is a complex emotional state involving chemical, cognitive, rewarding, and goal-directed behavioral components (S. Cacioppo & Hatfield, 2013; S. Cacioppo et al., 2012b). Contrary to love, lust is a state of intense sexual feelings/thoughts characterized by an interest or an increase in the frequency and the intensity of sexual thoughts/fantasies. Accordingly, sexual desire corresponds more to an urge that impels individuals to interact with others and initiate and/or to respond to sexual stimulation rather than a long-lasting emotional state as love can be (S. Cacioppo, 2017a; S. Cacioppo et al., 2012a for review).

To help participants differentiate between the two states, they were asked to make an immediate decision (judgment) during the task rather than more elaborated goals or development of feelings. More precisely, the participants were asked to indicate their intentions to feel love or lust for a person, not whether they felt love or lust. While feeling love for someone may take time, forming a judgment about an intention to love someone can occur much faster.

Methods

Participants

Twenty-two heterosexual male participants were included (*mean age*: 25.86 years; *SD* = 9.28).[1] All

[1]A total of 30 male subjects initially volunteered to participate in the present study, for which they received either $15 (or one course credit) for one hour of their time. Because of errors in recordings or poor signal-to-noise ratio in EEG data, recordings from two subjects were not included in the EEG data set analysis. In one instance, behavioral data was lost due to an error in the behavioral paradigm or experimenter. In another instance, a recording was excluded due to poor signal-to-noise ratio in the EEG data. Out of the remaining 28 participants, 24 of them described themselves as heterosexual, two as homosexual, one as pansexual, and one as bisexual. To keep the experimental group of participants homogeneous in terms of sexual orientation, only the participants with the sexual orientation that was the most representative of our sample was included in the present data set. Analyses focusing on individuals with a different sexual orientation (e.g., pansexual, homosexual, or bisexual) will be performed in the future as soon as a large enough sample of individuals with such sexual orientation will be collected. Out of the 24 remaining participants, data from two participants were not included in the final EEG analyses because of the poor signal-to-noise ratio in the EEG data, leaving the total sample to 22 subjects. Behavioral analyses were also performed on the same 22 subjects. However, raw data from three subjects could not be included in the stimulus-to-stimulus analyses as they were lost.

participants were native English speakers, undergraduate, graduate, or medical students at the University of Chicago. All had normal or corrected to-normal visual acuity. All participants were right-handed but one, as ascertained by the Edinburgh Handedness Inventory (Oldfield, 1971). None had any prior or current neurological or psychiatric impairment, as ascertained by a detailed anamnesis. On average, participants' feelings of loneliness (Russell, Peplau, & Cutrona, 1980), anxiety and depression (Zigmond & Snaith, 1983) were within normal ranges on all measures ($M_{loneliness}$ = 16.36, SD = 5.63; $M_{anxiety}$ = 7.41, SD = 2.74; $M_{depression}$ = 3.95, SD = 3.36). All participants provided oral informed consent to participate in the present study, which was approved by the Institutional Review Board (IRB) for the Protection of Human Subjects at the University of Chicago, Illinois.

Procedures

Subjects' instruction

Subjects were instructed to look at each photograph and decide as rapidly and precisely as possible whether they had the intention to be in a romantic relationship or lust (sexual desire) relationship with each individual. To make sure that all the subjects understood the concept of lust and romantic love in a similar manner, each subject received the following definitions: "*Sexual desire corresponds to a state of intense sexual feelings and/or sexual thoughts and/or sexual fantasies related to the image depicted in the photograph*"; while "*Romantic love corresponds to a state of intense and romantic longing for union with another depicted in the photograph*", at the beginning of the experiment. Moreover, the experimenter made clear to each participant that during the "romantic love" definition, the subject was requested to focus romantic feelings only, while during the "sexual desire" definition, they had to focus on lust only.

Experimental paradigm

All the subjects viewed a total of eight experimental blocks: Four experimental blocks with the romantic love instruction (Instruction A) and four experimental blocks with the lust instruction (Instruction B). The order of these instructions was counterbalanced across subjects using an ABBAABBA design. Each experimental block included the same 40 images that were repeated eight times, once in each of the eight blocks, with the order of the stimuli randomized across the trials. This entire behavioral experiment was carried out using E-Prime 2.0.8.90 software (Psychology Software Tools, Pittsburgh, PA).

Each block started with a 10-second baseline. In each block, each trial began with central presentation of a 1500–2500 ms (that was jittered with 100 ms increment) fixation cross. The target stimulus was then presented for 500 ms. Then, a blank ranking screen appeared until the subject responded (or up to 1500 ms). Finally, an eye-blink period (allowing the subject to blink) was presented for 1000 ms (Figure 1). This eye-blink period is suited to the EEG paradigm to avoid muscular eye-blink movements that contaminate the brain activity during the rest of the behavioral task.

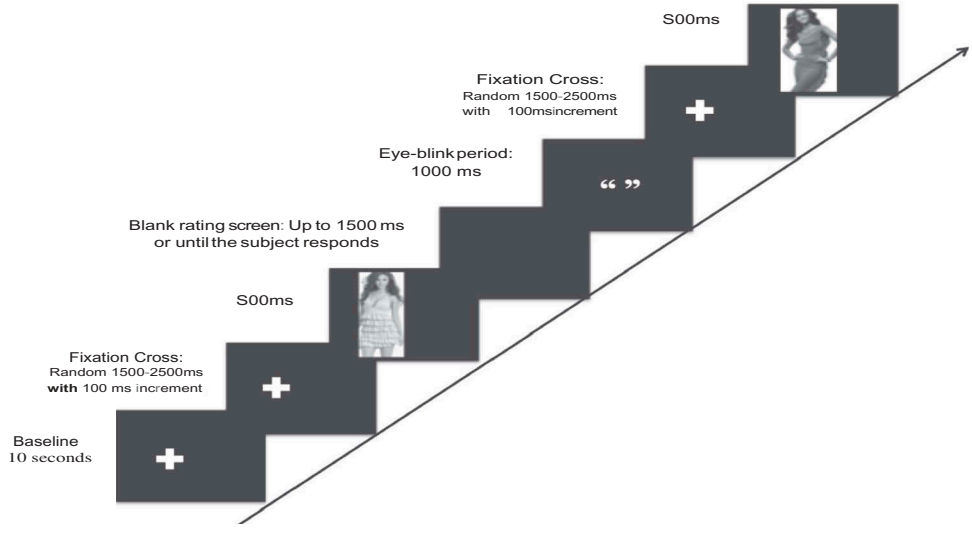

Figure 1. Experimental Paradigm. Each block started with a 10-second baseline. In each block, each trial began with a central presentation of a 1500–2500 ms (with 100 ms increment) fixation cross. The target stimulus was then presented for 500 ms. Then, a blank ranking screen appeared until the subject responded (or up to 1500 ms). Finally, an eye-blink period (allowing the subject to blink) was presented for 1000 ms (Figure 1). This eye-blink period is suited to the EEG paradigm to avoid muscular eye-blink movements that contaminate the brain activity during the rest of the behavioral task.

The participants were asked to respond "yes" or "no" by pressing eprime response keys with their index finger and middle finger of their right hand (one key per finger e.g., "yes" key to index finger, and "no" key to middle finger). To avoid any response bias that could have been attributed to the use of a specific finger for a specific response key, half of the participants were assigned to answer "yes" with their index finger, and "no" with the middle finger of their right hand. For the other half of the participants, the "yes" key was assigned to their middle finger, and the "no" key was assigned to the index finger of their right hand. No significant effect of the key assignment was found, which suggests there was no response bias in the present experiment.

Stimuli

The stimuli were a modified version of the stimuli presented in Bolmont et al.'s (2014). In the present study, all the photographs were scanned from female clothing magazines, in which women were not objectified in the photos. No nude images were included. As in Bolmont et al. (2014), the stimuli consisted of 40 photographs of female individuals who were gazing toward the camera. The photographs represented body models in the same age range as the subjects (19–41 years-old). To control for visual features across the stimuli, all photographs had the same size (182 × 405 pixels), and all were presented in the center of the monitor screen (Horizontal Visual Angle: 3.2°; Vertical Visual Angle: 5.4°), in grayscale with a white background.

Data acquisition and analysis

Continuous electroencephalogram (EEG) was recorded from 128 AgCl carbon-fiber coated electrodes using an Electric Geodesic Sensor Net® (HCGSN-128 channels with the Net Amps 400 amplifier; Electrical Geodesic Inc., Oregon; http://www.egi.com/), where EEG electrodes are arrayed in a dense and regular distribution across the head surface with an inter-sensor distance of approximately 3 cm. The EEG was digitized at 1000 Hz (corresponding to a sample bin of 1 ms), band-width at 0.01–200 Hz, with the vertex electrode (Cz) serving as an on-line recording reference; and impedances were kept below 100 kΩ. Behavioural performance was recorded from a Windows computer running E-Prime 2.0.8.90 software (Psychology Software Tools, Pittsburgh, PA). All subjects were seated in a comfortable chair about 110 cm away from a PC computer screen with their eyes levelled with the location of the stimuli that were presented in the center of that computer screen.

Electrophysiological image preprocessing

Electrophysiological data were imported and analyzed using EEGLAB (version 13.1.1; Arnauld Delorme and Scott Makeig, UCSD) and ERPLAB (version 4.0.2.3; Steve Luck and Javier Lopez-Calderon, University of California at Davis), with additional analysis done using Cartool (version 4.53; Denis Brunet; http://brainmapping.unige.ch/Cartool.htm). Electrical data were then down-sampled to 250 Hz (corresponding to a sample bin of 4 ms), band-pass filtered between 0.1 and 30 Hz, and notch filtered at 60 Hz to remove any residual interferences. Epochs of analysis were defined so as to end 500 ms after onset of visual stimuli, and contained a 100 ms pre-stimulus baseline. Epochs were visually inspected for oculomotor (saccades, and blinks), muscles, and other artifacts in addition to an automated threshold rejection criterion of 100 μV. Independent Component Analysis (ICA) weights were calculated to compute 128 components for each experimental block (using the RUNICA algorithm and EEGLAB functionality); these components were then visually inspected, and the datasets were purged of independent components related to eye blink artifacts. After off-line artifact rejections, surviving epochs of EEG were averaged for the 600 ms epoch length [−100 to +500 ms stimulus onset] for each participant to calculate the ERP for each condition. We equated the number of trials in the ERP of each condition by removing randomly trials from the lust condition so the average number of accepted trials for the romantic love condition was the same than that of the lust condition. Here, the ERP of the "Yes" responses included about 50 accepted trials in each condition (lust and romantic intentions, respectively). We equated the number of accepted trials in the ERPs to ensure that the same number of accepted trials was in the ERP of lust and in the ERP of romantic intentions. On average, the number of accepted trials was 50 for each condition for the "Yes" responses (i.e., romantic intentions or lustful intentions). For the "No" responses (i.e., intentions to not love or intentions to not lust), the number of accepted trials included in the ERP of each condition (lust and romantic love, respectively) was about 35 on average. Because the mean number of accepted trials for the "Yes" responses was not equated with that of the "No" responses, we did not compare the differential brain activity between "Yes" and "No" responses. Finally, ERPs were baseline corrected from −100 ms to 0, and channels with corrupted signals and channels showing substantial noise throughout the recording were interpolated to a standard 111-channel electrode array using a three-dimensional spline procedure (Perrin, Pernier, Bertnard, Giard, & Echallier, 1987).

Second-level electrophysiological analysis

These ERP data were subsequently processed for brain microsegmentation analyses using CENA (Chicago Electro NeuroImaging Analytics version 2015-Nov-11; S. Cacioppo, Balogh, & Cacioppo, 2015; S. Cacioppo & Cacioppo, 2015; S. Cacioppo et al., 2014b; https://hpenlaboratory.uchicago.edu/page/cena) microstate module in the Matlab-based EEG software Brainstorm 3.2 (Tadel, Baillet, Mosher, Pantazis, & Leahy, 2011). As per CENA standard procedure (S. Cacioppo et al., 2014b, 2015), four quantitative methods were applied to these ERP data across the 128-sensor space to detect brain microstates: (1) a root mean square error (RMSE) metric and a 99% confidence interval (CI) for identifying potential stable brain microstates; (2) a global field power (GFP) and a 99% CI for identifying changes in the overall level of activation of the brain; and (3) a similarity metric based on cosine distance and a 95% CI to determine whether template maps for successive brain microstates differ in configuration of brain activity, global field power, or a combination of the two; and (4) a bootstrapping procedure for assessing the extent to which the solutions identified in the micro-segmentation are robust and for empirically deriving additional experimental hypotheses (S. Cacioppo & Cacioppo, 2015; S. Cacioppo et al., 2014b).

As outlined in S. Cacioppo et al. (2014b, 2015), the present investigation focused on evoked brain microstates, as determined by a root mean square error (RMSE) metric using a lag of 12 ms, a baseline period from which to calculate the noise in the ERP configuration ranging from −100 ms pre-stimulus to 48 ms post-stimulus, and a 99% confidence interval (CI) for identifying potential stable brain microstates and for detecting significant rises or falls in the RMSE function. The series of potential brain microstates identified across an ERP waveform were then subjected to a cosine metric analysis using a 95% CI to determine whether the successive n + 1st microstate differed significantly in configuration from the nth microstate (see S. Cacioppo et al., 2014b for methodological details).

Statistical analysis plan

A priori orthogonal contrasts were conducted to determine differences in the evoked brain microstates elicited by the lust condition and the romantic love condition for the yes responses and the no responses, respectively. Here after, we described the procedure we used for the yes responses. A similar procedure was used for the no responses. The above brain microsegmentation routines were preformed using CENA, as follows: (1) The topographical maps (topo-maps) for the Grand Mean (i.e., waveform averaged across the romantic love condition and the lust condition) were again inspected for artifacts or bad channels in the recordings. [The Grand Mean is used because it generally represents the best estimate of integrity of the ERP recordings across time and it avoids any confirmatory bias in editing based on any expected differences between conditions.] Then, we created three other waveforms, as follows: (1) A group average waveform for the romantic intentions_yes condition; (2) A group average waveform for the lustful intentions_yes condition, and (3) A difference waveform of the group averages of (romantic love-lustful intentions_yes conditions or (1)–(2)); and (4) A Grand Mean waveform averaged across the romantic intentions_yes condition and lustful intentions_yes condition. Then, we applied CENA on (3) i.e., the difference waveform, to obtain the microsegmentation and the epochs of significant difference between romantic love and lust – that is, for the periods of time in which the brain microstates differed as a function of the task dimension (5). Then, we applied CENA on (1) to obtain the microsegmentation (and template maps) for romantic intentions_yes condition (6); on (2) to obtain the microsegmentation (and template maps) for lustful intentions_yes condition (7); and finally, we performed CENA on (4) to obtain the microsegmentation for the periods of time in which the evoked brain microstates did *not* differ as a function of the *task dimension* (8).

As described in CENA tutorial (S. Cacioppo & Cacioppo, 2015), we used the results of (5) to determine the epochs during which the evoked brain microstates in romantic love and lust differed statistically. For the epochs in which (5) shows *no* significant differences between (1) and (2), we use (8) to characterize the evoked brain microstates across *task dimension*. For such an epoch, distributed cortical source estimation (see below) was performed on the observed microstate(s) during this epoch in the Grand Mean (i.e., (8)). For the epochs in which (5) shows significant differences between (1) and (2), we used (6) and (7), respectively, to characterize the distinct evoked brain microstates as a function of *task dimension*. For such an epoch, source localization was performed on the observed microstate(s) during this epoch separately in (6) and in (7). A similar statistical plan was followed for intentions to not love and intentions to not lust.

Distributed cortical source estimation

As a final step, source localization of every identified stable evoked brain microstate described in the above was performed using the sLORETA EEG source computation method with head surface model created in Brainstorm with OpenMEEG BEM (Gramfort, Papadopoulo, Olivi, & Clerc, 2010; Kybic et al., 2005). Results were thresholded at 70% with a minimum size of 1 node, and 51% with a minimum size of 10. The anatomy model in Brainstorm, the Colin27 brain (Holmes et al.,

1998), was used in conjunction with MRI space software to automate the identification of source localization regions. Thresholded source regions were exported to MRI space for regional mapping using AFNI software (Cox, 1996). The AFNI tool was used to identify center of mass coordinates and specific overlap with anatomical regions using the stereotaxic Colin27 template.

Results

Behavioural results

Subjects reported more ($M_{yestolust\%}$ = 67.68%, SE = 3.25; $M_{yestolove\%}$ = 50.86%, SE = 4.62), p = .001), and faster lustful intentions than romantic intentions ($M_{yestolust\_reactiontimes}$ = 769.99 ms, SE = 55.35; $M_{yestolove\_reactiontimes}$ = 867.93 ms, SE = 62.10, p = .005). Reciprocally, intentions "not to love" were more frequent ($M_{notolove\%}$ = 47.32%, SE = 4.57) than intentions "not to lust" ($M_{notolust\%}$ = 32.32, SE = 3.25, p = .003). Analyses of reaction times did not reveal any significant differences ($M_{notolust\_reactiontimes}$ = 908.64 ms, SE = 55.23; $M_{notolove\_reactiontimes}$ = 953.56 ms, SE = 57.35, p = .15). Interestingly, a stimulus-by-stimulus analysis revealed that *about 62%* of the photographs that evoked a lustful intention also evoked an intention to engage in a romantic relationship (M = 61.69%, SD = 0.21; p = .0005), while only half of the photographs (M = 53.55%, SD = 0.24) evoking an intention to love also evoked a lustful intention.

Electrical neuroimaging results

Lustful intentions vs. romantically love

The *Chicago Electrical Neuroimaging Analytics* (CENA; S. Cacioppo, 2017b; S. Cacioppo & Cacioppo, 2015; S. Cacioppo et al., 2014b, 2015, 2016) revealed four brain microstates that were common to both lustful intentions and romantic intentions and only one different brain microstate in the 500 ms post-stimulus period (Figure 2). The first four microstates were common to both lustful intentions and romantic intentions, while the fifth microstate was specific to each intention. The windows of occurrence for these four common stable topographies corresponded to the following time intervals: Microstate 1: 96–136 ms (inclusive; mean GFP = 2.36^{10-7}, SD = 0.29^{10-7}), Microstate 2: 152–216 ms (inclusive; mean GFP = 1.71^{10-7}, SD = 0.23^{10-7}); Microstate 3: 248–276 ms (inclusive; mean GFP = 2.39^{10-7}, SD = 0.28^{10-7}); Microstate 4: 292–432 ms (inclusive; mean GFP = 3.93^{10-7}, SD = 0.18^{10-7}). After 432 ms post-stimulus onset, one additional discrete brain microstate followed the initial four common evoked brain microstates (see Figure 2). For the lustful intention condition, Microstate $5_{lust\_intention}$ occurred from 444 ms to 500 ms (mean GFP = 3.24^{10-7}, SD = 0.06^{10-7}) i.e., 16 ms earlier than the fifth brain microstate evoked in the romantic romantic intention condition. Microstate $5_{love\_intention}$ occurred from 460 ms to 500 ms (mean GFP = 3.54^{10-7}, SD = 0.07^{10-7}). As suggested from prior studies, a GFP peak was observed at 124 ms post-stimulus onset (amplitude: 2.65^{10-7}), and another GPF peak was observed at 304 ms post-stimulus onset (amplitude: 3.70^{10-7}) for lustful intention, and at 304 ms post-stimulus onset (amplitude: 4.18^{10-7}) for intention to romantically love.

Between-subjects bootstrap analyses were performed to investigate the robustness of each brain microstate across participants. The first four microstates, which were elicited 0–432 ms post-stimulus and were common across Conditions, were investigated using 7315 bootstrapped ERPs based on the Grand Mean ERPs, with each bootstrap ERP representing data from a unique randomly selected set of 80% of the participants. Results indicated the identification of the brain microstates to be from generally robust, with a peak (microstate onset) of the bootstrapped runs identified within ±10% of microstate onset for: (a) Microstate 1 in 99.7% of the bootstrap runs, (b) Microstate 2 in 96.6% of the runs, (c) Microstate 3 in 83.5% of the runs, and (d) Microstate 4 in 83.5% of the runs.

Because the microstates after 432 ms differed across conditions, these were investigated using 7315 bootstrapped ERPs based on the mean ERPs within each condition, with each bootstrap ERP representing data from a unique randomly selected set of 80% of the participants. Microstate 5 occurred in 46.8% of the bootstrap runs for lustful intentions, and in 94.2% of the bootstrap runs for romantic intentions. In terms of GPF peaks, the bootstrap results revealed that GFP peaked at 124 ms in 100% of the runs, and at 304 ms post-stimulus for in 99.9% of the runs for lustful intentions and in 100% of the runs for romantic intentions.

Source localization estimation were then performed for exploratory purposes (see Table 1A and B). Source localization estimation of the four brain microstates that were common to both the lust and the romantic intentions (Table 1A) revealed the recruitment of the visual cortex and brain areas associated with social attention and emotional processes (e.g., superior parietal lobe, anterior cingulate, insula, precuneus, amygdala, cingulate cortex), as well as brain areas involved face and body processing (fusiform gyrus), self-other mental association (e.g., angular gyrus, superior temporal gyrus), and intention (e.g., inferior frontal gyrus; Table 1A).

What distinguished lustful intention from romantic intentions was the specific distributed *set* of cortical

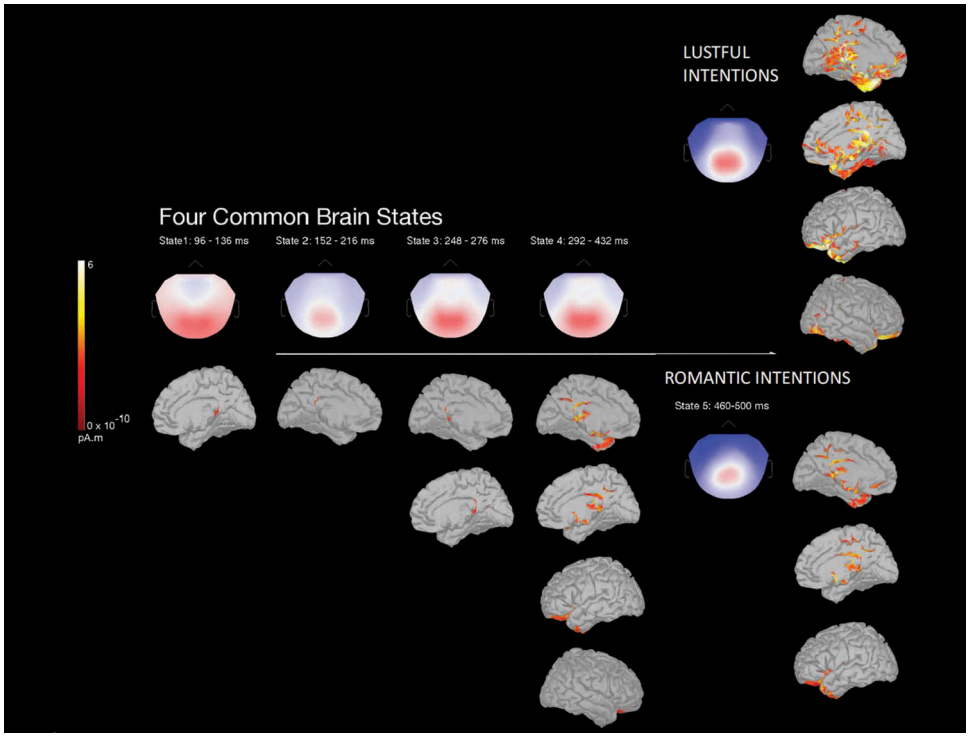

Figure 2. Brain microstates and source localization cortical surface maps for the five microstates evoked during lustful intentions vs. romantic intentions. The topographic maps are shown with the nasion upward and left scalp leftward. Blue areas depict negative potentials and red areas depict positive potentials. Specific source localization regions are detailed in Table 1.

regions that was estimated to characterize the fifth brain microstate in each condition (see Table 1B). While each specific brain states at this later stage include common brain areas, such as brain areas involved in intention processing (e.g., the left inferior frontal gyrus, left inferior parietal lobule), emotional processing (e.g., ventral posterior cingulate gyrus), and highly integrated operations, such as self-processing and empathy (e.g., precuneus; Cavana & Trimble, 2006), each specific brain states had also a unique signature. For lustful intentions, Microstate 5 was characterized by an additional and specific activation of two brain areas involved in the mirror neuron system i.e., the right inferior frontal gyrus (Brodmann area, BA 47) and the reactivation of the right angular gyrus (BA 39), a brain area that was activated in Microstate 2 i.e., between 152–216 ms post-stimulus onset. For romantic intentions, on the other hand, Microstate 5 was characterized by activation of brain areas known to be activated in love (e.g., anterior insula, S. Cacioppo et al., 2013a; Table 1B).

Intentions to not lust vs. not romantically love

For intentions to not lust or not to romantically love, only the first two brain microstates (until 240 ms post-stimulus onset) were common to both conditions, while the last three brain microstates were specific to each condition (Figure 3). The windows of occurrence for the common two brain microstates corresponded to the following time intervals: Microstate 1: 96–136 ms (inclusive; mean GFP = 2.33^{10-7}, *SD* = 0.29^{10-7}); Microstate 2: 160–216 ms (inclusive; mean GFP = 1.63^{10-7}, *SD* = 0.26^{10-7}).

Then, for intentions to not lust, the windows of occurrence for each specific brain microstate corresponded to the following time intervals: Microstate $3_{nottolust\_intention}$: 244–272 ms (inclusive; mean GFP = 2.45^{10-7}, *SD* = 0.24^{10-7}); Microstate $4_{nottolust\_intention}$: 292–428 ms (inclusive; mean GFP = 3.65^{10-7}, *SD* = 0.21^{10-7}); Microstate $5_{nottolust\_intention}$: 464–500 ms (inclusive; mean GFP = 3.35^{10-7}, *SD* = 0.02^{10-7}). For intentions to not romantically love, the three specific brain microstates occurred at the following time intervals: Microstate $3_{nottolove\_intention}$: 248–276 ms (inclusive; mean GFP = 2.53^{10-7}, *SD* = 0.30^{10-7}); Microstate $4_{nottolove\_intention}$: 296–440 ms (inclusive; mean GFP = 3.55^{10-7}, *SD* = 0.27^{10-7}); Microstate $5_{nottolove\_intention}$: 484–500 ms (inclusive; mean GFP = 3.18^{10-7}, *SD* = 0.01^{10-7}). A GFP peak was observed at 128 ms post-stimulus onset (amplitude: 2.62^{10-7}) and another GPF peak was observed at 304 ms post-stimulus onset (amplitude: 4.01^{10-7}) for intention to not lust, and at 308 ms post-stimulus onset (amplitude: 4.07^{10-7}) for intention to not romantically love.

Table 1. Source localization regions for the five microstates evoked during lustful intentions vs. romantic intentions. Source localization regions for brain microstates common to both intention types are presented in Table 1A, while source localization regions for brain microstates specific to each intention type are presented in Table 1B.

Table 1A

Sheet1

State 1 (Common)	Vol (ul)	x	y	z	pA.m
L/R Parahippocampal Gyrus	**12,248**	**5.1**	**−46.8**	**3.6**	**1.10E-010**
L/R Culmen					
L/R Lingual Gyrus					
L/R Posterior Cingulate L Cingulate Gyrus					
R Cuneus					
R Precuneus					
BA 18, 19, 27, 29, 30, 31, 36					
Left Primary Visual Cortex (BA 17)	**1282**	**−9.7**	**−70.4**	**17.3**	**9.60E-011**
L Posterior Cingulate L Cuneus					
BA 18, 30, 31					
L Associative Visual Cortex (BA 19)	**497**	**−23.4**	**−56.3**	**−12.7**	**9.40E-011**
L Parahippocampal Gyrus L Culmen					
L Angular Gyrus (BA 39)	**419**	**−46.4**	**−64.8**	**20.2**	**8.40E-011**
L Angular Gyrus L BA 19					
R Associative Visual Cortex (BA 19)	**393**	**43.9**	**−79.4**	**7.4**	**9.00E-011**
R Middle Temporal Gyrus BA 39					
L Fusiform Gyrus (BA 37) L Parahippocampal Gyrus L Culmen	**366**	**−42.3**	**−37.2**	**−25.6**	**8.70E-011**
L BA 36					
State 2 (Common)	Vol (ul)	x	y	z	pA.m
L/R Posterior Cingulate	**11,804**	**0.4**	**−56.1**	**17.3**	**9.20E-011**
L/R Cingulate Gyrus L/R Cuneus					
L/R Precuneus					
R Posterior Cingulate BA 17, 18, 23, 30, 31					
L Inferior Frontal Gyrus (BA 47)	**1963**	**−26.3**	**17.9**	**−21.1**	**7.50E-011**
L Inferior Frontal Gyrus L Medial Frontal Gyrus L Rectal Gyrus					
L Subcallosal Gyrus L Orbital Gyrus					
BA 11, 13, 25, 38					
R Angular Gyrus (BA 39)	**1544**	**46**	**−65.6**	**21.2**	**9.90E-011**
R Angular Gyrus BA 19					
R Associative Visual Cortex (BA 19)	**864**	**44**	**−79.3**	**5.3**	**9.20E-011**
R Middle Temporal Gyrus					
L Precuneus (BA 7)	**837**	**−7.4**	**−55.1**	**48.7**	**9.30E-011**
L Ventral Tegmental Area	**785**	**−14.1**	**−14.1**	**−14.5**	**7.70E-011**
BA 28					
L Associative Visual Cortex (BA 19)	**759**	**−23.6**	**−55**	**−9.7**	**9.00E-011**
L Fusiform Gyrus					
R Dorsal Posterior Cingulate Cortex (BA 31)	**707**	**4.9**	**−56.6**	**42.5**	**9.80E-011**
BA 7					
R Superior Parietal Lobule	**602**	**38.2**	**−64.6**	**51.1**	**8.40E-011**
BA 7					
R Posterior Insula	**497**	**40**	**−21**	**12.1**	**7.30E-011**
BA 13					
L Dorsal Posterior Cingulate Cortex (BA 31)	497	−9.9	−35.8	53.6	8.50E-011
BA 5					
R Supramarginal Gyrus R Inferiori Parietal Lobule BA 40	**393**	**49.7**	**−54.8**	**37.2**	**7.70E-011**
R Fusiform Gyrus (BA 37)	**366**	**22.9**	**−58.2**	**−10.6**	**8.00E-011**
R Lingual Gyrus R Culmen					
BA 19					
R Visual Associative Cortex (BA 18)	**340**	**20.7**	**−77**	**−8.5**	**8.70E-011**
State 3 (Common)	Vol (ul)	x	y	z	pA.m
L Inferior Frontal Gyrus	**11,961**	**−23.4**	**9.4**	**−21.6**	**1.2e-10**
L Superior Temporal Gyrus L Parahippocampal Gyrus L Medial Frontal Gyrus					
L Rectal Gyrus L Uncus					
L Middle Temporal Gyrus L Middle Frontal Gyrus					
L Insula					
L Orbital Gyrus L Amygdala					
BA 11, 13, 21, 25, 28, 34, 38, 47					
L/R Posterior Cingulate Cortex	**3376**	**−2.2**	**−44.2**	**14.3**	**1.2e-10**
L/R Cingulate Gyrus					
L/R Parahippocampal Gyrus BA 29, 30, 31					
R Inferior Frontal Gyrus (BA 47)	**3141**	**21.6**	**22.9**	**−21.6**	**1.1e-10**
R Superior Temporal Gyrus R Rectal Gyrus					
R Orbital Gyrus					
R Middle Frontal Gyrus R Subcallosal Gyrus					
R Medial Frontal Gyrus BA 11					

(*Continued*)

Table 1. (Continued).

Table 1A

Sheet1

L/R Anterior Cingulate Cortex L/R Medial Frontal Gyrus BA 10, 32	**2853**	**0.9**	**44.9**	**8.3**	**1.1e-10**
R Primary Visual Cortex (BA 17) R Precuneus R Posterior Cingulate R Lingual Gyrus BA 18, 19, 30, 31	**2460**	**9.8**	**−72.1**	**13.6**	**1.1e-10**
L Primary Visual Cortex (BA 17) L Posterior Cingulate L Cuneus BA 30, 31	**1439**	**−12.2**	**−68.3**	**15.5**	**1.2e-10**
R Angular Gyrus (BA 39)	**1021**	**45.5**	**−65.8**	**21.2**	**1.1e-10**
L Associative Visual Cortex (BA 19) L Fusiform Gyrus L Lingual Gyrus	**837**	**−24.1**	**−55.3**	**−9.8**	**1.3e-10**
L Inferior Frontal Gyrus (BA 45) BA 47	**628**	**−44.8**	**20.2**	**4.8**	**9.9e-11**
R Associative Visual Cortex (BA 19)	**576**	**43.5**	**−79.2**	**3.8**	**1.0e-10**
L Precuneus (BA 7)	**471**	**−6.8**	**−54.7**	**48.4**	**1.2e-10**
R Ventral Anterior Cingulate Cortex (BA 24) R Paracentral Lobule R Cingulate Gyrus BA 6	**471**	**2.8**	**−12**	**50.4**	**1.1e-10**
L Inferior Parietal Lobule L Superior Temporal Gyrus L Transverse Temporal Gyrus BA 41	**445**	**−45.3**	**−29.9**	**16.2**	**8.8e-11**
L Fusiform Gyrus (BA 37) L Parahippocampal Gyrus L Culmen BA 20, 36	**419**	**−42.1**	**−38.4**	**−24.8**	**9.9e-11**
L Fusiform Gyrus (BA 37)	**340**	**−44**	**−57.4**	**−19.3**	**1.1e-10**
State 4 (Common)	Vol (ul)	x	y	z	pA.m
L Inferior Frontal Gyrus L Superior Temporal Gyrus L Insula L Parahippocampal Gyrus L Medial Frontal Gyrus L Rectacl Gyrus L Middle Temporal Gyrus L Uncus L Middle Frontal Gyrus L Subcallosal Gyrus L Amygdala BA 11, 13, 25, 38, 47	**15,075**	**−22.4**	**9.3**	**−19.1**	**1.7e-10**
L/R Cingulate Gyrus (BA 30) L/R Posterior Cingulate L/R Parahippocampal Gyrus L/R Precuneus BA 29, 31	**4973**	**−4**	**−39.6**	**18.4**	**1.8e-10**
R Inferior Frontal Gyrus (BA 47) R Superior Temporal Gyrus R Rectal Gyrus R Orbital Gyrus R Medial Frontal Gyrus BA 11, 38	**2643**	**20.3**	**22.1**	**−22.9**	**1.5e-10**
L Precuneus (BA 7)	**1806**	**−7.6**	**−59.3**	**46.9**	**1.6e-10**
L Inferior Parietal Lobule L Superior Temporal Gyrus L Transverse Temporal Gyrus BA 13, 41	**1544**	**−43.8**	**−26.3**	**13.5**	**1.5e-10**
L Supplementary Motor Area (BA 6) L Precentral Gyrus L Superior Temporal Gyrus BA 13, 22	**968**	**−46**	**0.1**	**9.1**	**1.4e-10**
L Dorsal Anterior Cingulate Cortex (BA 32)	**785**	**−5**	**28.4**	**−8**	**1.5e-10**
R Precuneus (BA 7)	**785**	**5.3**	**−57.9**	**42.2**	**1.9e-10**
L Dorsal Posterior Cingulate Cortex (BA 31) BA 5	**628**	**−8.8**	**−36.1**	**53.7**	**1.8e-10**
L Thalamus	**602**	**−4.3**	**−27.8**	**−6.4**	**1.5e-10**
R Visual Associative Area (BA 18) BA 31	**550**	**13.4**	**−68.2**	**17.4**	**1.5e-10**
L Ventral Posterior Cingulate Cortex (BA 23) BA 30	**497**	**−14.4**	**−61.5**	**7.9**	**1.6e-10**
R Paracentral Lobule BA 5, 6	**497**	**4.9**	**−39.1**	**60**	**1.6e-10**
L Associative Visual Cortex (BA 19)	**366**	**−23.4**	**−55.3**	**−9.6**	**1.5e-10**
R Ventral Posterior Cingulate Cortex (BA 23) BA 30	**366**	**18.2**	**−58.3**	**8.7**	**1.4e-10**

Table 1B

State 5 (Lust)	Vol (ul)	x	y	z	pA.m
L Inferior Frontal Gyrus L Superior Temporal Gyrus L Parahippocampal Gyrus L Medial Frontal Gyrus L Rectal Gyrus L Insula L Middle Temporal Gyrus L Uncus L Middle Frontal Gyrus L Subcallosal Gyrus L Orbital Gyrus BA 11, 13, 38, 47	**15,625**	**−22.1**	**9.3**	**−20.5**	**1.5e-10**

(*Continued*)

Table 1. (Continued).

Table 1B

L/R Cingulate Gyrus (BA 30)	**4816**	**−4.7**	**−40.3**	**17.9**	**1.5e-10**
L/R Posterior Cingulate					
L/R Parahippocampal Gyrus					
R Inferior Frontal Gyrus (BA 47)	**3873**	**21.9**	**24.6**	**−21.6**	**1.3e-10**
R Superior Temporal Gyrus R Rectal Gyrus					
R Middle Frontal Gyrus R Medial Frontal Gyrus R Orbital Gyrus					
R Subcallosal Gyrus BA 11					
L Precuneus (BA 7)	**1675**	**−7.6**	**−58.6**	**47.3**	**1.3e-10**
R Visual Associative Cortex (BA 18)	**759**	**13.8**	**−68.2**	**17.2**	**1.3e-10**
R Cuneus					
R Posterior Cingulate BA 31					
R Dorsal Posterior Cingulate Cortex (BA 31)	**759**	**5.3**	**−57.4**	**42.3**	**1.6e-10**
BA 7					
R Dorsal Anterior Cingulate Cortex (BA 32)	**733**	**6.1**	**39.7**	**8.8**	**1.2e-10**
L Dorsal Posterior Cingulate Cortex (BA 31)	**602**	**−9**	**−35.8**	**53.7**	**1.5e-10**
BA 5					
L Ventral Posterior Cingulate Gyrus (BA 23)	**523**	**−14.5**	**−62.1**	**7.6**	**1.3e-10**
BA 30	**497**	**−6.2**	**48.8**	**9.9**	**1.2e-10**
L Dorsal Anterior Cingulate Cortex (BA 32)					
L Anterior Cingulate BA 10					
R Angular Gyrus (BA 39)	**497**	**45.3**	**−65.7**	**22.4**	**1.3e-10**
R Paracentral Lobule	**471**	**5**	**−39**	**60.1**	**1.3e-10**
R Superior Temporal Gyrus (BA 38)	**445**	**35.6**	**18.5**	**−41.1**	**1.2e-10**
L Anterior Cingulate Cortex (BA 32)	**419**	**−4.5**	**25.8**	**−9.3**	**1.3e-10**
L Associative Visual Cortex (BA 19)	**393**	**−23.4**	**−55.7**	**−10**	**1.2e-10**
L Fusiform Gyrus					
L Inferior Parietal Lobule (BA 40)	**340**	**−41.7**	**−34.9**	**17**	**1.2e-10**
L Insula BA 41					

State 5 (Love)	Vol (ul)	x	y	z	pA.m
L Inferior Frontal Gyrus	**13,321**	**−28.7**	**9.7**	**−17.5**	**1.90E-010**
L Insula					
L Superior Temporal Gyrus L Parahippocampal Gyrus L Medial Frontal Gyrus					
L Middle Temporal Gyrus L Precentral Gyrus					
L Uncus					
L Rectal Gyrus					
L Middle Frontal Gyrus L Subcallosal Gyrus					
L Inferior Temporal Gyrus					
L/R Posterior Cingulate Cortex (BA 30)	**3455**	**−6.3**	**−38.8**	**10.7**	**1.90E-010**
L Parahippocampal Gyrus BA 23, 29					
L/R Anterior Cingulate Cortex (BA 32)	**1963**	**−3.6**	**32.6**	**−5.3**	**1.70E-010**
BA 11, 24					
L Inferior Parietal Lobule (BA 40)	**1911**	**−43.9**	**−25.2**	**13**	**1.80E-010**
L Superior Temporal Gyrus					
L Transverse Temporal Gyrus L Postcentral Gyrus					
BA 13, 22, 41					
L/R Ventral Posterior Cingulate Gyrus (BA 23)	**1884**	**−1.6**	**−35.9**	**34.7**	**2.00E-010**
L/R BA 31					
Ventral Tegmental Area	**1544**	**7.2**	**−7.1**	**−11.5**	**1.80E-010**
R Amygdala BA 25					
L Precuneus (BA 7)	**1518**	**−7.9**	**−60.8**	**44.5**	**2.00E-010**
L Thalamus	**916**	**−4.1**	**−27.1**	**−8.9**	**1.80E-010**
R Precuneus (BA 7)	**811**	**5.2**	**−60.1**	**41.7**	**2.30E-010**
L Dorsal Posterior Cingulate Cortex (BA 31)	**811**	**−8.2**	**−35.8**	**54**	**1.90E-010**
BA 5					
R Sensory Associative Cortex	**680**	**5**	**−41.2**	**58.9**	**1.80E-010**
BA 5					
R Dorsal Posterior Cingulate Cortex (BA 31)	**602**	**12.5**	**−67.4**	**21.6**	**1.60E-010**
L Visual Associative Cortex (BA 18)	**550**	**−8.8**	**−78.7**	**32.3**	**1.50E-010**
L Precuneus BA 19					
R Supplementary Motor Area (BA 6)	**523**	**5.1**	**−23.6**	**57.2**	**1.60E-010**
L Mid-Insula	**497**	**−46.6**	**−6.9**	**10.1**	**1.70E-010**
L Precentral Gyrus BA 13					
R Anterior Insula (BA 13)	**419**	**34.8**	**16**	**−7.4**	**1.50E-010**
BA 47					
L Superior Temporal Gyrus (BA 38)	**340**	**−44.6**	**18.5**	**−32.3**	**1.80E-010**

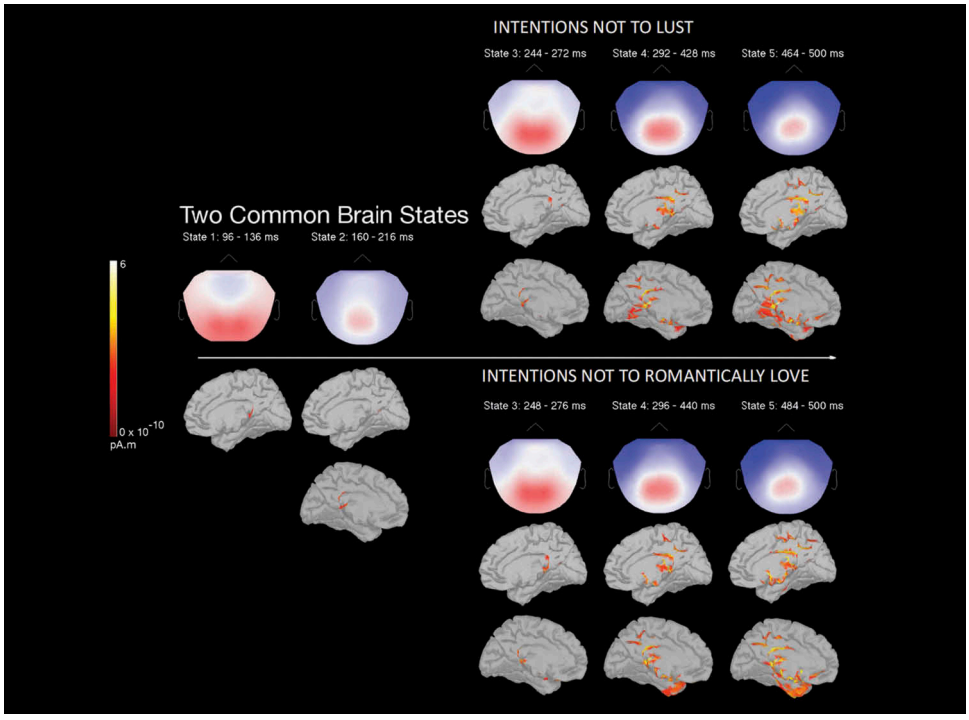

Figure 3. Brain microstates and source localization cortical surface maps for the five microstates evoked during intentions to not lust vs. to not romantically love. The topographic maps are shown with the nasion upward and left scalp leftward. Blue areas depict negative potentials and red areas depict positive potentials. Specific source localization regions are detailed in Table 2.

Between-subjects bootstrap analyses were also performed to investigate the robustness of each brain microstate across participants using the same procedure than that describe above. The first two microstates were investigated using 7315 bootstrapped ERPs based on the Grand Mean ERPs, with each bootstrap ERP representing data from a unique randomly selected set of 80% of the participants. Results indicated the identification of the brain microstates to be from generally robust, with a peak (microstate onset) of the bootstrapped runs identified within ±10% of microstate onset for: (a) the first microstate in 100% of the bootstrap runs, (b) the second microstate onset in 100% of the runs.

Because the microstates after 240 ms differed across conditions, these were investigated using 7315 bootstrapped ERPs based on the mean ERPs within each condition, with each bootstrap ERP representing data from a unique randomly selected set of 80% of the participants. The bootstrap results for the additional brain microstates evoked in each condition indicated generally robust microstate identification, with a microstate onset of the bootstrapped runs identified within ±10% of microstate onset for each brain microstate, as follows: Microstate 3 occurred in 100% of the bootstrap runs for the intention not to lust, and in 94.4% of the bootstrap runs for the intentions not to love; Microstate 4 occurred in 100% of the bootstrap runs for the intention not to lust, and in 94.4% of the bootstrap runs for the intentions not to love; and Microstate 5 occurred in 100% of the bootstrap runs for the intention not to lust, and in 41.1% of the bootstrap runs for the intentions not to love. In terms of GPF peaks, the bootstrap results revealed that GFP peaked at 128 ms in 99.9% of the runs, and at 304 ms post-stimulus for the intentions not to lust in 100% of the runs and at 308 ms post-stimulus onset for intentions to not love in 100% of the runs.

Source localization estimation were then performed for exploratory purposes (See Table 2A–C). Source localization estimation of the two brain microstates that were common to both intentions to not lust and not romantically love (Table 2A) revealed the recruitment of the visual cortex and brain areas associated with intentions (e.g., angular gyrus), decision making (orbitofrontal cortex), face/body processing, and associative memory, and past somatosensory experiences (posterior insula). After 240 ms, each intention type was characterized by a specific activations of brain areas (Table 2B and C). For instance, intentions to not love were characterized by activations of brain areas involved in associative memory, while intentions to not lust were characterized by activations of brain areas involved in anxiety and social threat processing.

Table 2. Source localization regions for the five microstates evoked during intentions to not lust vs. intentions to not romantically love. Source localization regions for brain microstates common to both intention types are presented in Table 2A, while source localization regions for brain microstates specific to each intention type are presented in Table 2B (intentions to not lust) and Table 2C (intentions to not romantically love).

Table 2A

State 1 (Common)	Vol (ul)	x	y	z	pA.m
L/R Posterior Cingulate Gyrus L/R Parahippocampal Gyrus L/R Posterior Cingulate Right Cuneus Right Lingual Gyrus Right Precuneus BA 18, 19, 27, 30, 31	**10,940**	**3.1**	**−45**	**4.1**	**9.7e-11**
L Primary Visual Cortex (BA 17) L Posterior Cingulate BA 18, 30, 31	**916**	**−9.9**	**−69.2**	**18**	**8.7e-11**
R Cingulate Gyrus (BA 8) R Anterior Cingulate BA 32	**576**	**5.9**	**16.7**	**37.4**	**7.8e-11**
L Angular Gyrus (BA 39) L Superior Temporal Gyrus L Angular Gyrus BA 19	**445**	**−46.6**	**−64.8**	**20**	**8.0e-11**
R Associative Visual Cortex (BA 19) R Middle Temporal Gyrus BA 39	**340**	**43.9**	**−79**	**6.9**	**8.2e-11**
R Supplementary Motor Area (BA 6) R Paracentral Lobule R Cingulate Gyrus BA 31, 24	**340**	**4.9**	**−14.1**	**54.8**	**8.6e-11**
L Fusiform Gyrus (BA 37)	**314**	**−43.7**	**−56.3**	**−18.2**	**8.4e-11**
R Parahippocampal Gyrus R Amygdala BA 34	**314**	**24.8**	**−10.5**	**−16.2**	**7.4e-11**
L Paracentral Lobule BA 5, 6	**314**	**−9.6**	**−34.8**	**53.7**	**8.1e-11**
State 2 (Common)	Vol (ul)	x	y	z	pA.m
L/R Dorsal Posterior Cingulate Cortex (BA 31) L/R Cuneus L/R Cingulate Gyrus L/R Precuneus L Lingual Gyrus L Parahippocampal Gyrus BA 17, 18, 19, 23, 30, 31	**11,646**	**−1.7**	**−59.3**	**13.5**	**1.0e-10**
R Angular Gyrus (BA 39) R Angular Gyrus R Superior Temporal Gyrus R BA 19	**995**	**44.9**	**−65.3**	**22**	**1.1e-10**
L Superior Temporal Gyrus L Inferior Frontal Gyrus BA 38, 47	**968**	**−34.7**	**15.3**	**−22.4**	**9.4e-11**
L Precuneus (BA 7)	**785**	**−7.1**	**−56.8**	**46**	**9.9e-11**
L Orbito-frontal Gyrus (BA 11) L Inferior Frontal Gyrus L Rectal Gyrus L Orbital Gyrus BA 25, 47	**759**	**−12.1**	**26.5**	**−20.5**	**8.8e-11**
R Dorsal Posterior Cingulate Cortex (BA 31) R Cingulate Gyrus BA 7	**602**	**4.9**	**−57.5**	**41.9**	**1.0e-10**
R Associative Visual Cortex (BA 19) R Lingual Gyrus	**576**	**23.1**	**−58.3**	**−10.2**	**9.8e-11**
R Posterior Insula R Superior Temporal Gyrus BA 13, 41	**419**	**40.1**	**−22.1**	**8.7**	**8.5e-11**
L Paracentral Lobule BA 5	**314**	**−9.5**	**−35.2**	**53.3**	**9.4e-11**
L Parahippocampal Gyrus BA 27	**288**	**−27**	**−30.7**	**−8.7**	**9.1e-11**

Table 2B

State 3 (Lust)	Vol (ul)	x	y	z	pA.m
L/R Visual Associative Cortex (BA 18) L/R Posterior Cingulate L/R Lingual Gyrus L/R Precuneus L/R Parahippocampal Gyrus L/R Cingulate Gyrus L Fusiform Gyrus BA 17, 19, 23, 31	14,316	−6	−59.2	5	1.1e-10
L Superior Temporal Gyrus L Parahippocampal Gyrus L Inferior Frontal Gyrus L Medial Frontal Gyrus L Medial Temporal Gyrus L Middle Frontal Gyrus L Insula L Orbital Gyrus BA 11, 13, 21, 25, 28, 34, 38, 47	**12,641**	**−26.5**	**8.3**	**−21.3**	**1.1e-10**
L Orbito-frontal Gyrus (BA 11) R Parahippocampal Gyrus R Superior Temporal Gyrus R Middle Frontal Gyrus R Orbital Gyrus R Superior Frontal Gyrus R Medial Frontal Gyrus BA 25, 28, 34, 38, 47	**6334**	**20.3**	**13.6**	**−19.2**	**1.0e-10**
L/R Anterior Cingulate L/R Medial Frontal Gyrus BA 9, 10, 24, 32	**3376**	**2**	**44**	**8.2**	**1.0e-10**
L Supplementary Motor Area (BA 6) L Paracentral Lobule L Cingulate Gyrus BA 5, 24, 31	**2853**	**1**	**−19.4**	**51.9**	**9.3e-11**

(*Continued*)

Table 2. (Continued).

Table 2B

R Angular Gyrus (BA 39) R BA 19	**1125**	**45.5**	**−65.6**	**20.1**	**1.0e-10**
L Inferior Frontal Gyrus (BA 45) L Antrior Insula L Precentral Gyrus BA 13, 47	**1073**	**−43.9**	**19.9**	**5.6**	**9.8e-11**
L Dorsal Posterior Cingulate Cortex (BA 31) L Precuneus L Postcentral Gyrus BA 5, 7	**837**	**−9.5**	**−39.4**	**55.3**	**9.7e-11**
R Associative Visual Cortex (BA 19) R Inferior Occipital Gyrus R Middle Temporal Gyrus BA 139	707	43.7	−79.3	2.9	9.7e-11
L Precuneus (BA 7)	**680**	**−7**	**−54.6**	**49**	**1.1e-10**
L Inferior Parietal Lobule L Superior Temporal Gyrus L Transverse Temporal Gyrus BA 13, 41	**628**	**−43.3**	**−30.3**	**17**	**8.4e-11**
R Supplementary Motor Area (BA 6) R Medial Frontal Gyrus BA 32	**550**	**5.2**	**10.4**	**42.4**	**9.5e-11**
L Middle Temporal Gyrus (BA 21) L BA 20	**393**	**−58.9**	**−38.1**	**−21.8**	**8.7e-11**
L Supplementary Motor Area (BA 6) L Insula L Precentral Gyrus BA 13, 22	**366**	**−49.3**	**1**	**5.1**	**8.3e-11**
R Precuneus (BA 7) BA 5	**340**	**8.1**	**−47.3**	**56.2**	**8.8e-11**
State 4 (Lust)	Vol (ul)	x	y	z	pA.m
Left Inferior Frontal Gyrus Left Superior Temporal Gyrus Left Medial Frontal Gyrus Left Insula Left Parahippocampal Gyrus Left Orbital Gyrus BA 11, 13, 25, 28, 38, 47	**7250**	**−25.9**	**9.1**	**−14.9**	**1.6e-10**
L/R Posterior Cingulate Cortex L/R Cuneus R Precuneus L Lingual Gyrus L Parahippocampal Gyrus L Fusiform Gyrus BA 18, 19, 23, 29, 30, 31	**6517**	**−4.2**	**−51.1**	**8.5**	**1.7e-10**
L Precuneus (BA 7) L Postcentural Gyrus	**1832**	**−7.7**	**−59.4**	**46.7**	**1.8e-10**
L/R Ventral Posterior Cingulate Cortex (BA 23) L/R Posterior Cingulate BA 31	**1649**	**−1.8**	**−40.5**	**33**	**1.8e-10**
L Inferior Parietal Lobule L Superior Temporal Gyrus L Transverse Temporal Gyrus BA 13, 14	**1518**	**−43.4**	**−26.4**	**13.5**	**1.6e-10**
R Ventral Tegmental Area	**1413**	**12.2**	**−12.1**	**−13.6**	**1.7e-10**
L Middle Temporal Gyrus L Superior Temporal Gyrus L BA 21, 38	**1256**	**−39.6**	**8.8**	**−40.4**	**1.6e-10**
R Inferior Frontal Gyrus (BA 47) R Superior Temporal Gyrus R Orbital Gyrus BA 11, 38, 47	**1152**	**20.6**	**23.3**	**−25.6**	**1.4e-10**
R Precuneus (BA 7)	**785**	**5.1**	**−58.5**	**42**	**2.0e-10**
L Dorsal Posterior Cingulate Cortex (BA 31) BA 5	**654**	**−8.8**	**−36.2**	**53.8**	**1.9e-10**
L Culmen L Fusiform Gyrus	**523**	**−29.9**	**−52.2**	**−21.8**	**1.4e-10**
R Paracentral Lobule BA 5, 6	**523**	**4.7**	**−39.3**	**60**	**1.5e-10**
L Primary Motor Cortex L Precentral Gyrus BA 6, 13	**393**	**−46.4**	**−7.4**	**10**	**1.4e-10**
L Visual Associative Area (BA 18) L Cuneus BA 7, 19	**393**	**−11.5**	**−75.3**	**29.8**	**1.3e-10**
L Dorsal Anterior Cingulate Cortex (BA 32)	**340**	**−4.5**	**28.4**	**−8.5**	**1.5e-10**
State 5 (Lust)	Vol (ul)	x	y	z	pA.m
Left Inferior Frontal Gyrus Left Superior Temporal Gyrus Left Medial Frontal Gyrus Left Insula Left Parahippocampal Gyrus Left Precentral Gyrus L Rectal Gyrus L Amygdala BA 11, 13, 25, 38, 45, 47	**7747**	**−28.7**	**8.8**	**−11.7**	**1.8e-10**
L Posterior Cingulate (BA 30) L Lingual Gyrus L Parahippocampal Gyrus L Cuneus L Culmen R Posterior Cingulate L Fusiform Gyrus BA 18, 19, 23, 29	**5182**	**−8**	**−43.4**	**6.8**	**1.8e-10**

(*Continued*)

Table 2. (Continued).

Table 2B

L Middle Temporal Gyrus L Superior Temporal Gyrus BA 21, 38	**1989**	**−38**	**4.8**	**−41.4**	**1.7e-10**
L/R Ventral Posterior Cingulate Cortex (BA 23)	**1963**	**−1.6**	**−38**	**33.8**	**2.0e-10**
R Visual Associative Cortex (BA 18)	**1780**	**13.6**	**−66.6**	**17.3**	**1.6e-10**
R Posterior Cingulate R Cuneus					
BA 30, 31					
L Precuneus (BA 7)	**1596**	**−7.8**	**−61.1**	**44.5**	**2.1e-10**
R Parahippocampal Gyrus	**1466**	**11.7**	**−10.6**	**−12.9**	**1.8e-10**
R Amygdala					
L Posterior Insula	**1309**	**−43.7**	**−21.7**	**11.1**	**1.8e-10**
L Superior Temporal Gyrus					
L Transverse Temporal Gyrus L Postcentral Gyrus					
BA 13, 22, 41					
L/R Dorsal Anterior Cingulate Cortex (BA 32)	**1152**	**−4.2**	**32.7**	**−5.1**	**1.6e-10**
R Precuneus (BA 7)	**890**	**5.5**	**−60.4**	**41.6**	**2.3e-10**
L Secondary Visual Cortex (BA 18)	**837**	**−9.1**	**−78.3**	**31.2**	**1.6e-10**
L Precuneus					
L Paracentral Lobule	**785**	**−8.5**	**−35.9**	**54**	**2.0e-10**
BA 5					
R Paracentral Lobule	**707**	**4.9**	**−41.4**	**59**	**1.7e-10**
BA 5					
R Supplementary Motor Area (BA 6)	**602**	**5**	**−22.5**	**57.5**	**1.6e-10**
R Anterior Insula (BA 13)	**523**	**34.9**	**15.5**	**−8.1**	**1.6e-10**
BA 47					
L posterior Superior Temporal Gyrus	**497**	**−43.4**	**−35.7**	**16.6**	**1.6e-10**
L Insula L BA 41					
L Primary Motor Area	**419**	**−46.6**	**−7.1**	**9.9**	**1.6e-10**
L Precentral Gyrus BA 6, 13					
R Orbito-frontal Gyrus (BA 11)	**340**	**15.4**	**32.6**	**−24.4**	**1.4e-10**
R Orbital Gyrus BA 47					

Table 2C

State 3 (Love)	Vol (ul)	x	y	z
L Inferior Frontal Gyrus	**13,086**	**−25.8**	**11.5**	**−19.9**
L Superior Temporal Gyrus L Insula				
L Medial Frontal Gyrus L Rectal Gyrus				
L Parahippocampal Gyrus L Middle Temporal Gyrus L Middle Frontal Gyrus				
L Orbital Gyrus L Amygdala				
BA 11, 13, 25, 38, 47				
L/R Posterior Cingulate L/R Parahippocampal Gyrus L/R Cingulate Gyrus	**3926**	**−2.8**	**−43**	**11.1**
BA 27, 29, 30, 31				
L/R Anterior Cingulate L/R Medial Frontal Gyrus BA 10, 24, 32	**2225**	**0.9**	**45.1**	**5.8**
R Inferior Frontal Gyrus (BA 47)	**1335**	**21.4**	**21.6**	**−26.1**
R Orbital Gyrus R Rectal Gyrus BA 11, 38				
R Primary Visual Cortex (BA 17)	**759**	**11.1**	**−65.7**	**13.5**
R Precuneus BA 30, 31				
L Primary Visual Cortex (BA 17)	**707**	**−10.9**	**−68.8**	**19.5**
L Posterior Cingulate BA 31				
R Associative Visual Cortex (BA 19)	**654**	**45.1**	**−66**	**21.1**
BA 39				
R Inferior Frontal Gyrus (BA 47)	**602**	**35.4**	**30**	**−13.3**
R Secondary Visual Cortex (BA 18)	**576**	**11.8**	**−76.3**	**27.1**
R Precuneus BA 31				
L Thalamus	**523**	**−5.1**	**−27.7**	**−6.9**
R Orbito-frontal Gyrus (BA 11)	**366**	**3**	**21.8**	**−24.5**
L Fusiform Gyrus (BA 37)	**340**	**−43.5**	**−56.1**	**−18.5**
L Precuneus (BA 7)	**340**	**−6.9**	**−54.7**	**47.3**
State 4 (Love)	Vol (ul)	x	y	z
L Inferior Frontal Gyrus	**16,986**	**−24.3**	**7.8**	**−17.5**
L Insula				
L Superior Temporal Gyrus L Parahippocampal Gyrus L MediaLFrontal Gyrus				
L Rectal Gyrus				
L Middle Temporal Gyrus L Uncus				
L Middle Frontal Gyrus L Precentral Gyrus				
L Subcallosal Gyrus L Amygdala				
BA 11, 13, 25, 38, 47				
L/R Posterior Cingulate (BA 30)	**3900**	**−6.9**	**−41.6**	**10.4**
L/R Parahippocampal Gyrus R Posterior Cingulate				
BA 23, 29				
L Precuneus (BA 7)	**1884**	**−7.6**	**−59.3**	**46.9**

(*Continued*)

Table 2. (Continued).

Table 2C

L/R Ventral Posterior Cingulate Cortex (BA 23) L/R Posterior Cingulate L/R Precuneus BA 24, 31	**1727**	**−1.8**	**−40**	**33.2**
L Inferior Parietal Lobule L posterior Superior Temporal Gyrus L Transverse Temporal Gyrus L Postcentral Gyrus BA 13, 22, 41, 43	**1596**	**−44.6**	**−25.9**	**13.5**
R Inferior Frontal Gyrus (BA 47) R Superior Temporal Gyrus R Orbital Gyrus BA 11, 38	**1047**	**20.5**	**22.8**	**−26**
R Precuneus (BA 7)	**837**	**5.3**	**−58.6**	**42.1**
R Secondary Visual Cortex (BA 18) R Cuneus R Posterior Cingulate BA 30, 31	**733**	**14.2**	**−68.5**	**16.9**
L Dorsal Posterior Cingulate Cortex (BA 31) Ba 5	**654**	**−8.7**	**−36.2**	**53.8**
R Paracentral Lobule BA 5, 6	**550**	**4.7**	**−39.6**	**59.9**
L Dorsal Anterior Cingulate Cortex (BA 32) L Subcallosal Gyrus L/R Medial Frontal Gyrus	**497**	**−4.2**	**25.4**	**−10.2**
R Ventral Posterior Cingulate Cortex (BA 23) BA 30	**366**	**16.3**	**−58.7**	**9**
L Secondary Visual Cortex (BA 18) L Cuneus BA 7, 19	**366**	**−10.5**	**−76.2**	**30.9**
State 5 (Love)	Vol (ul)	x	y	z
L Inferior Frontal Gyrus L Insula L Superior Temporal Gyrus L Parahippocampal Gyrus L Medial Frontal Gyrus L Middle Temporal Gyrus L Precentral Gyrus L Uncus L Rectal Gyrus L Middle Frontal Gyrus L Culmen L Subcallosal Gyrus L Inferior Temporal Gyrus L Amygdala BA 11, 13, 25, 38, 47	**16,253**	**−28.6**	**6.8**	**−18.4**
L Thalamus L/R Posterior Cingulate L Hippocampus BA 29, 30	**5156**	**−10.1**	**−34.6**	**2.7**
L/R Ventral Posterior Cingulate Cortex (BA 23) BA 24, 31	**1806**	**−1.6**	**−35.7**	**34.9**
L Precuneus (BA 7)	**1492**	**−7.9**	**−60.9**	**44.5**
L Posterior Insula L Superior Temporal Gyrus L Transverse Temporal Gyrus L Postcentral Gyrus BA 13, 22, 41	**1335**	**−44.6**	**−21.6**	**12**
R Parahippocampal Gyrus	**1073**	**6.4**	**−8.8**	**−11.6**
R Secondary Visual Cortex (BA 18) R Cuneus BA 31	968	11	−71.3	23.7
R Precuneus (BA 7)	**837**	**5.2**	**−60.4**	**41.7**
R Paracentral Lobule BA 5	**785**	**5.2**	**−41.9**	**58.8**
L Paracentral Lobule BA 5, 6	**759**	**−8.3**	**−35.7**	**53.9**
L Dorsal Anterior Cingulate Cortex (BA 32)	**707**	**−5.5**	**28.7**	**−8.1**
L Secondary Visual Cortex (BA 18) L Precuneus BA 7, 19	**654**	**−7.7**	**−79.5**	**32.2**
R Hippocampus R Amygdala	**628**	**25.6**	**−6.6**	**−20.5**
R Supplementary Motor Area (BA 6) R Paracentral Lobule	**576**	**4.9**	**−23.4**	**57.7**
L Inferior parietal lobule L posterior Superior Temporal Gyrus BA 13, 41	**419**	**−43.2**	**−35.7**	**16.6**

Discussion

In the present study, a total of 22 healthy heterosexual male participants' electrical brain activity was collected while they completed a computerized social intention task in which they were asked to view photographs of strangers and decide whether they had the intention to be (or not to be) in a lustful relationship or a romantic relationship with each individual. Our behavioral results showed that men report more and faster lustful intentions than romantic intentions.

Our high-density electrical neuroimaging results expanded these behavioral results by showing that both types of intentions were characterized by similar as well as different functional brain states. Specifically, our neuroimaging results first showed considerable overlaps among lustful intentions and romantic intentions during the first 432 ms post-stimulus period. This finding is in accord with our behavioral findings showing that 62% of the lustful intentions were also romantic intentions. This finding is consistent with prior work in social psychology and neuroscience suggesting that romantic love may grow out of lust (S. Cacioppo, 2017a; S. Cacioppo & Cacioppo, 2013; S. Cacioppo & Hatfield, 2013; S. Cacioppo et al., 2012b). This prior work and related research have shown that there are commonalities between the women whom men find sexually desirable and the women whom men find potentially lovable. Prior research also suggests, for instance, that the strongest relationship – passionate love – involves activation of the home bases of both love and lust (S. Cacioppo, 2017a; S. Cacioppo et al., 2012a, 2012b), and that the intention (i.e., short-term sexual relationship, committed long-term romantic relationship) activates partially but not entirely overlapping brain regions and triggers different patterns of eye-tracking data. For instance, intentions regarding sexual desire are associated with activity in the posterior insula, whereas intentions regarding romantic love are associated with activity in the anterior insula. We were able to find a patient in Argentina who had a localized lesion in the anterior insula (S. Cacioppo et al., 2013a). When tested using this paradigm, this patient showed impaired behavioral performance when making judgments about love but not when making judgments about sexual desire even though the images for the two judgments were the same (S. Cacioppo et al., 2013a). Together these results suggest that the functional brain states we identified in the current study reflect the intention rather than the stimulus per se. If there are differences between the intentions toward the partially overlapping states of love and lust, there are undoubtedly differences between these intentions and other social intentions. The extent to which the common microstates identified in the current study will generalize to other social intentions is a matter for future research to determine.

While the focus of the present study was not on gender differences, we encourage future studies that aim to test whether women show similar behavioral results than men. Given ample research suggesting gender differences with respect to romantic goals, attachment styles, their own concepts of "romance" and the strength of their associations between sex and romance, we expect future studies on gender differences, social intentions, and brain dynamics to identify behavioral patterns and brain microstates characterizing intentions to lust that are specific to men only and others specific to women only. Moreover, because we recently showed brain microstates and hemispheric specialization may vary in women as a function of their menstrual cycle (S. Cacioppo et al., 2013b) and the fact that sexual desire increases during certain phases of the menstrual cycle for some women (Regan, 1996, 1999), we recommend future studies test lust and love intentions in pre-menopausal women who are normally cycling during all the different phases of their menstrual cycle. Nevertheless, because prior correlational analyses, eye-tracking studies, and neuroimaging studies have also shown many similar patterns between love and lust among both women and men (Bolmont et al., 2014; Hendrick & Hendrick, 1995), we also consider that a possible alternative hypothesis is that common brain microstates would be observed in both men and women. In other words, future studies need to consider both gender differences and similarities in lust and love intentions within intimate relationships.

The present overlaps between intentions to love and intentions to lust are also in line with: (1) psychological theories that suggest overlaps between the concept/construct of love and that of lust, such as the awareness of wanting (or wishing) to attain a potentially pleasurable goal that is currently unattainable or uncertain (Hatfield & Rapson, 2009); (2) our recent eye-tracking study that showed both similar and distinct visual patterns for romantic love and lust (Bolmont et al., 2014; S. Cacioppo, 2016 for review); (3) prior EEG/ERP studies (e.g., S. Cacioppo, Grafton, & Bianchi-Demicheli, 2012c; Ortigue & Bianchi-Demicheli, 2008) and prior fMRI studies (see S. Cacioppo et al., 2012a for meta-analyses) that showed neural overlaps between love and lust within the cortical areas involved in self-representation, goal-directed actions, and body image (middle frontal gyrus, superior temporal gyrus, temporo-parietal

junction, and occipito-temporal cortices) and within subcortical brain areas associated with positive emotions, euphoria, reward, motivation and addiction (e.g., striatum, thalamus, hippocampus, anterior cingulate cortex, & ventral tegmental area; S. Cacioppo & Hatfield, 2013; S. Cacioppo et al., 2012a).

From a neural viewpoint, the brain source localizations estimated here were performed for exploratory purposes. It is important to note, nevertheless, that the CENA quantitative procedure we used for identifying each stable event-related brain microstate that led to these brain source localization provides a better basis for source localization estimates than previous software of electrical neuroimaging, in part because CENA differentiates functional brain microstates from transition (noisy) states and improves signal-to-noise ratio for each functional brain microstate and related source localization (S. Cacioppo, 2017b; S. Cacioppo et al., 2014b). Our results revealed that both intention types were sustained by similar activations of the inferior frontal gyrus and the inferior parietal lobule/angular gyrus for the first 432 ms after stimulus onset, as well as within the visual cortex and brain areas associated with social attention and emotional processes (e.g., superior parietal lobe, anterior cingulate, insula, precuneus, amygdala, cingulate cortex), and brain areas involved face and body processing (fusiform gyrus).

What distinguished lustful intentions from romantic intentions was in a specific distributed *set* of cortical regions of the fifth functional brain state in each condition (around 430 ms post-stimulus onset). Interestingly, Microstate 5 occurred 16 ms earlier for lustful intentions than that for romantic intentions. The delay in the fifth microstate and significantly longer reaction time for romance-yes intentions, as compared to lust-yes intentions, may reflect the consideration of the greater and longer-term implications of a committed romantic relationship or by a need for more cognitive elaboration in construing romance intentions than lust intentions. For lustful intentions, Microstate 5 was characterized by a specific activation of two brain areas involved in the right inferior frontal gyrus (Brodmann area, BA 47) and the right angular gyrus (BA 39), a brain area that was also activated in Microstate 2 i.e., between 152–216 ms post-stimulus onset. For romantic intentions, Microstate 5 was characterized by activation of brain areas known to be activated in love (e.g., anterior insula, S. Cacioppo et al., 2013a). These results, showing the involvement of limbic areas as well as higher-order cognitive brain areas in the early and later stage of information processing, are in line with the top-down neuro-functional model of goal-directed social relationship, which suggest influences of past self-related cognitive experiences on emotional feelings and goal-directed social behaviours at both an early stage processing (e.g., more unconscious and automatic) and a later stage processing (e.g., more consciously controlled and elaborative).

These results are in line with theories in social psychology suggesting that romantic love and lust are distinctive states that have been assumed not to differ in their valence as much as in their short-term or long-term goals (S. Cacioppo & Cacioppo, 2013; Diamond, 2004; Diamond & Dickenson, 2012; Hatfield & Rapson, 2005, 2009; Komisaruk & Whipple, 1998). Whereas both romantic love and lust call for mechanisms underlying the awareness of wanting (or wishing) to attain a potentially pleasurable goal that is currently unattainable, lust is oriented toward consummation of a *sexual* (rather than romantic) encounter and an increase in wanting (or wishing) to attain a *short-term* (rather than long-term) pleasurable goal, while romantic love is characterized by the wanting (or wishing) to maintain a *long-lasting romantic* relationship with a specific other with whom one would share encounters beyond sex (Hatfield & Rapson, 2009). Consistent with this notion, one could regard lustful intentions as being related to decision making about *short-term* goals, whereas romantic intentions would be related to decision-making about more *long-term* goals. Moreover, intentions regarding lust involve short-term commitments and fewer consequences than intentions regarding romantic love. For instance, a romantic relationship is more likely to constrain future sexual or romantic relationships than is a sexual encounter. This suggest that the present behavioral differences between love and lust intentions likely reflect a lower threshold for engaging in a relatively inconsequential sexual encounter than for engaging in a long-term romantic relationship. This distinction is in accord with the present electrical neuroimaging results of the current study, as well. The early microstates for the two intentions were similar but the intention to form a romantic relationship was characterized by an additional, later microstate, perhaps reflecting the longer time-frame over which love, in contrast to lustful, intentions have consequences. To further address these questions, future studies might investigate whether intentions to commit to a short-term vs. long-term relationship call for similar brain states and spatio-temporal dynamics than those evoked by lustful intentions and romantic intentions.

Interestingly, intentions to not love vs. not lust were characterized by differential activations at 240 ms post-stimulus. Source localization estimation of the two brain microstates prior to 240 ms (i.e., two brain microstates common to both intentions to not lust and not romantically love) revealed the recruitment of the visual cortex

and brain areas associated with intentions, decision making (orbitofrontal cortex), face/body processing, and associative memory, and integrated past somatosensory experiences (posterior insula). Then, after 240 ms poststimulus, each intention type was characterized by its specific brain network and chronoarchitecture. For instance, intentions to not love were characterized by activations of brain areas involved in associative memory, while intentions to not lust were characterized by activations of brain areas involved in anxiety and social threat processing. The inferior fronto-parietal network was activated differently over time, as a function of the intention type. Together, these results suggest that the mirror neuron system may not only code for the motor correlates of intentions, but also for the social meaning of intentions and its valence at both early/automatic and later/more elaborative stages of information processing.

Acknowledgments

The authors thank the participants and members and alumni from the High-Performance Electrical Neuroimaging Laboratory at the University of Chicago. This research was partly funded by Valeant Grant# 2016-1301.

Disclosure statement

No potential conflict of interest was reported by the authors.

Funding

This work was supported by the Valeant Pharmaceuticals International [2016-1301].

References

Allison, T., Puce, A., & McCarthy, G. (2000). Social perception from visual cues: Role of the STS region. *Trends in Cognitive Sciences*, *4*, 267–278.

Argyle, M., & Cook, M. (1976). *Gaze and mutual gaze*. Cambridge, UK: Cambridge University Press.

Baron-Cohen, S. (1995). *Mindblindness: An essay on autism and theory of mind*. Cambridge, MA: MIT Press.

Bolmont, M., Cacioppo, J. T., & Cacioppo, S. (2014). Love is in the gaze: An eye-tracking study of love and sexual desire. *Psychological Science*, *25*, 1748–1756.

Cacioppo, S. (2017a, August 30). Neuroimaging of female sexual desire and hypoactive sexual desire disorder. *Sexual Medicine Reviews*, *5*, 434–444.

Cacioppo, S. (2016). Neural markers of interpersonal attraction: A possible new direction for couple's therapy. In A. Scarantino (Ed.), Emotion Researcher, *ISRE's sourcebook for research on emotion and affect*. [accessed 2017 October 24]. Retrieved from: http://emotionresearcher.com/how-to-cite-er/

Cacioppo, S., Balogh, S., & Cacioppo, J. T. (2015). Implicit attention to negative social, in contrast to nonsocial, words in the Stroop task differs between individuals high and low in loneliness: Evidence from event-related brain microstates. *Cortex*, *70*, 213–233.

Cacioppo, S., Bangee, M., Balogh, S., Cardenas-Iniguez, C., Qualter, P., & Cacioppo, J. T. (2016). Loneliness and implicit attention to social threat: A high-performance electrical neuroimaging study. *Cognitive Neuroscience*, *7*, 138–159.

Cacioppo, S., Bianchi-Demicheli, F., Bischof, P., DeZiegler, D., Michel, C. M., & Landis, T. (2013b). Hemispheric specialization varies with EEG brain resting states and phase of menstrual cycle. *PLoS One*, *8*, e63196.

Cacioppo, S., Bianchi-Demicheli, F., Frum, C., Pfaus, J. G., & Lewis, J. W. (2012a). The common neural bases between sexual desire and love: A multilevel kernel density fMRI analysis. *The Journal of Sexual Medicine*, *9*(4), 1048–1054.

Cacioppo, S., Bianchi-Demicheli, F., Hatfield, E., & Rapson, R. L. (2012b). Social neuroscience of love. *Clinical NeuroPsychiatry*, *9*, 3–13.

Cacioppo, S., & Cacioppo, J. T. (2013). Lust for life. *Nature Scientific American Mind*, *24*, 56–60.

Cacioppo, S., & Cacioppo, J. T. (2015). Dynamic spatiotemporal brain analyses using high-performance electrical neuroimaging, part II: A step-by-step tutorial. *Journal of Neuroscience Methods*, *256*, 184–197.

Cacioppo, S., Couto, B., Bolmont, M., Sedeno, L., Frum, C., Lewis, J. W., … Cacioppo, J. T. (2013a). Selective decision-making deficit in love following damage to the anterior insula. *Current Trends in Neurology*, *7*, 15–19.

Cacioppo, S., Fontang, F., Patel, N., Decety, J., Monteleone, G., & Cacioppo, J. T. (2014a). Intention understanding over T: A neuroimaging study on shared representations and tennis return predictions. *Frontiers in Human Neuroscience*, *8*, 781.

Cacioppo, S., Grafton, S. T., & Bianchi-Demicheli, F. (2012c). The speed of passionate love, as a subliminal prime: A high-density electrical neuroimaging study. *NeuroQuantology*, *10*, 715–724.

Cacioppo, S., & Hatfield, E. (2013). Passionate love and sexual desire. In P. Whelehan & A. Bolin (Eds.), *Encyclopedia of human behavior*. New York, NY: Wiley.

Cacioppo, S. (2017b). High-performance electrophysiological microsegmentation and brain source localization. In J. T. Cacioppo, L. Tassinary, & G. Berntson (Eds.), *Handbook of psychophysiology* (4th ed.). Cambridge: Cambridge University Press.

Cacioppo, S., Juan, E., & Monteleone, G. (2017). Predicting intentions of a familiar significant other beyond the mirror neuron system. *Frontiers in Behavioral Neuroscience*, *11*, 155. doi:10.3389/fnbeh.2017.00155

Cacioppo, S., Weiss, R. M., Runesha, H. B., & Cacioppo, J. T. (2014b). Dynamic spatiotemporal brain analyses using high performance electrical neuroimaging: Theoretical framework and validation. *Journal of Neuroscience Methods*, *238*, 11–34.

Cattaneo, L., Fabbri-Destro, M., Boria, S., Pieraccini, C., Monti, A., Cossu, G., & Rizzolatti, G. (2007). Impairment of actions chains in autism and its possible role in intention understanding. *Proceedings of the National Academy of Sciences*, *104*, 17825–17830.

Cavanna, A. E. (2006). The precuneus: A review of its functional anatomy and behavioural correlates. *Brain*, *129*(Pt 3), 564–583.

Cox, R. W. (1996). AFNI: Software for analysis and visualization of functional magnetic resonance neuroimages. *Computers and Biomedical Research*, *29*, 162–173.

Cunnington, R., Windischberger, C., Robinson, S., & Moser, E. (2006). The selection of intended actions and the observation of others' actions: A time-resolved fMRI study. *Neuroimage*, *29*, 1294–1302.

Diamond, L. M. (2004). Emerging perspectives on distinctions between romantic love and sexual desire. *Current Directions in Psychological Science*, *13*, 116–119.

Diamond, L. M., & Dickenson, J. A. (2012). The neuroimaging of love and desire: Review and future directions. *Clinical Neuropsychiatry*, *9*, 39–46.

Emery, N. J. (2000). The eyes have it: The neuroethology, function and evolution of social gaze. *Neuroscience & Biobehavioral Reviews*, *24*, 581–604.

Fogassi, L., Ferrari, P. F., Gesierich, B., Rozzi, S., Chersi, F., et al. (2005). Parietal lobe: From action organization to intention understanding. *Science*, *308*, 662–667.

Friston, K., & Frith, C. (2015). A duet for one. *Consciousness and Cognition*, *36*, 390–405.

Gallese, V., Fadiga, L., Fogassi, L., & Rizzolatti, G. (1996). Action recognition in the premotor cortex. *Brain*, *119*, 593–609.

Grafton, S. T. (2009). Embodied cognition and the simulation of action to understand others. *Annals of the New York Academy of Sciences*, *1156*, 97–117.

Gramfort, A., Papadopoulo, T., Olivi, E., & Clerc, M. (2010). OpenMEEG: Open source software for quasi-static bioelectromagnetics. *Biomedical Engineering Online*, *9*, 45.

Hamilton, A. F., & Grafton, S. T. (2008). Action outcomes are represented in human inferior fronto-parietal cortex. *Cerebral Cortex*, *18*, 1160–1168.

Hatfield, E., & Rapson, R. L. (2005). *Love and sex: Cross-cultural perspectives*. Lanham, MD: University Press of America.

Hatfield, E., & Rapson, R. L. (2009). The neuropsychology of passionate love and sexual desire. In E. Cuyler & M. Ackhart (Eds.), *Psychology of social relationships*. Hauppauge, NY: Nova Science.

Hendrick, S. S., & Hendrick, C. (1987). Love and sexual attitudes, self-disclosure and sensation seeking. *Journal of Social and Personal Relationships.*, *4*, 281–297.

Hendrick, S. S., & Hendrick, C. (1995). Gender differences and similarities in sex and love. *Personal Relationships*, *2*(1), 55–65.

Holmes, C.J., Hoge., R, Collins, L., Woods, R., Toga, A.W., & Evans, A.C. (1998). Enhancement of MR images using registration for signal averaging. *Journal of Computer Assisted Tomography*, *22*(2), 324–333. doi:10.1097/00004728-199803000-00032

Honaga, E., Ishii, R., Kurimoto, R., Canuet, L., Ikezawa, K., Takahashi, H., … Takeda, M. (2010). Post-movement beta rebound abnormality as indicator of mirror neuron system dysfunction in autistic spectrum disorder: An MEG study. *Neuroscience Letters*, *478*, 141–145.

Iacoboni, M., Molnar-Szakacs, I., Gallese, V., Buccino, G., Mazziotta, J. C., Rizzolatti, G., & Ashe, J. (2005). Grasping the intentions of others with one's own mirror neuron system. *PLoS Biology*, *3*, e79.

Jones, B. C., Main, J. C., DeBruine, L. M., Little, A. C., & Welling, L. L. (2010). Reading the look of love: Sexually dimorphic cues in opposite-sex faces influence gaze categorization. *Psychological Science*, *21*(6), 796–798.

Juan, E., Frum, C., Bianchi-Demicheli, F., Wang, Y., Lewis, J. W., & Cacioppo, S. (2013). Beyond human intentions and emotions. *Frontiers in Human Neuroscience*, *7*, 99.

Komisaruk, B. R., & Whipple, B. (1998). Love as sensory stimulation: Physiological consequences of its deprivation and expression. *Psychoneuroendocrinology*, *23*, 927–944.

Kybic, J., Clerc, M., Abboud, T., Faugeras, O., Keriven, R., & Papadopoulo, T. A. (2005). A common formalism for the integral formulations of the forward EEG problem. *IEEE Transactions on Medical Imaging*, *24*, 12–28.

Land, M. F., & Lee, D. N. (1994). Where we look when we steer. *Nature*, *369*, 742–744.

Land, M. F., Mennie, N., & Rusted, J. (1999). The roles of vision and eye movements in the control of activities of daily living. *Perception*, *28*, 1311–1328.

Lehmann, D. (1987). Principles of spatial analysis. In A. S. Gevins & A. Remond (Eds.), *Handbook of electroencephalography and clinical neurophysiology, vol. 1. Methods of analysis of brain electrical and magnetic signals* (pp. 309–354). Amsterdam: Elsevier.

Lewis, J. W. (2006). Cortical networks related to human use of tools. *Neuroscientist*, *12*, 211–231.

Majdandžić, J., Grol, M. J., van Schie, H. T., Verhagen, L., Toni, I., & Bekkering, H. (2007). The role of immediate and final goals in action planning: An fMRI study. *Neuroimage*, *37*, 589–598.

Murray, M. M., Brunet, D., & Michel, C. M. (2008). Topographic ERP analyses: A step-by-step tutorial review. *Brain Topography*, *20*, 249–264.

Oldfield, R. C. (1971). The assessment and analysis of handedness: The Edinburgh inventory. *Neuropsychologia*, *9*, 97–113.

Ortigue, S., & Bianchi-Demicheli, F. (2008). The chronoarchitecture of human sexual desire: A high-density electrical mapping study. *NeuroImage*, *43*, 337–345.

Ortigue, S., Bianchi-Demicheli, F., Patel, N., Frum, C., & Lewis, J. W. (2010a). Neuroimaging of love: FMRI meta-analysis evidence toward new perspectives in sexual medicine. *The Journal of Sexual Medicine*, *7*, 3541–3552.

Ortigue, S., Michel, C. M., Murray, M. M., Mohr, C., Carbonnel, S., & Landis, T. (2004). Electrical neuroimaging reveals early generator modulation to emotional words. *Neuroimage*, *21* (4), 1242–1251.

Ortigue, S., Sinigaglia, C., Rizzolatti, G., & Grafton, S. T. (2010b). Understanding actions of others: The electrodynamics of the left and right hemispheres. A high-density EEG neuroimaging study. *PLoS One*, *5*, e12160.

Ortigue, S., Thompson, J. C., Parasuraman, R., & Grafton, S. T. (2009). Spatio-temporal dynamics of human intention understanding in temporo-parietal cortex: A combined EEG/fMRI repetition suppression paradigm. *PLoS One*, *4*, 6962.

Perrin, F., Pernier, J., Bertnard, O., Giard, M. H., & Echallier, J. F. (1987). Mapping of scalp potentials by surface spline interpolation. *Electroencephalography and Clinical Neurophysiology*, *66*, 75–81.

Ramnani, N., & Miall, R. C. (2004). A system in the human brain for predicting the actions of others. *Nature Neuroscience*, *7*, 85–90.

Regan, P. C. (1996). Rhythms of desire: Association between menstrual cycle phases and female sexual desire. *The Canadian Journal of Human Sexuality*, *5*, 145–156.

Regan, P. C. (1998). Of lust and love: Beliefs about the role of sexual desire in romantic relationships. *Personal Relationships*, *5*, 139–157.

Regan, P. C. (1999). Hormonal correlates and causes of sexual desire: A review. *The Canadian Journal of Human Sexuality*, *8*, 1–16.

Regan, P. C., & Berscheid, E. (1999). *Lust: What we know about human sexual desire*. Thousand Oaks, CA: Sage; Sage series on close relationships.

Rizzolatti, G., Fadiga, L., Gallese, V., & Fogassi, L. (1996). Premotor cortex and the recognition of motor actions. *Cognitive Brain Research*, *3*, 131–141.

Rizzolatti, G., & Sinigaglia, C. (2007). Mirror neurons and motor intentionality. *Functional Neurology*, *22*, 205–210.

Rizzolatti, G., & Sinigaglia, C. (2008). Further reflections on how we interpret the actions of others. *Nature*, *455*, 589.

Rizzolatti, G., & Sinigaglia, C. (2010). The functional role of the parieto-frontal mirror circuit: Interpretations and misinterpretations. *Nature Reviews Neuroscience*, *11*, 264–274.

Rupp, H. A., & Wallen, K. (2007). Sex differences in viewing sexual stimuli: An eye-tracking study in men and women. *Hormones and Behavior*, *51*, 524–533.

Russell, D, Peplau, L. A, & Cutrona, C. E. (1980). The revised ucla loneliness scale: concurrent and discriminant validity evidence. *Journal Of Personality And Social Psychology*, *39*, 472-480. doi:10.1037/0022-3514.39.3.472

Tadel, F., Baillet, S., Mosher, J. C., Pantazis, D., & Leahy, R. M. (2011). Brainstorm: A user-friendly application for MEG/EEG analysis. *Computational Intelligence and Neuroscience*, *2011*, 1–13.

Tennov, D. (1998). *Love and limerence: The experience of being in love*. Lanham, MD: Scarborough House.

Toni, I., Thoenissen, D., & Zilles, K. (2001). Movement preparation and motor intention. *Neuroimage*, *14*, S110–S117.

Van der Cruyssen, L., Van Duynslaeger, M., Cortoos, A., & Van Overwalle, F. (2009). ERP time course and brain areas of spontaneous and intentional goal inferences. *Social Neuroscience*, *4*, 165–184.

Van Duynslaeger, M., Van Overwalle, F., & Verstraeten, E. (2007). Electrophysiological time course and brain areas of spontaneous and intentional trait inferences. *Social Cognitive and Affective Neuroscience*, *2*, 174–188.

Vistoli, D., Passerieux, C., El Zein, M., Clumeck, C., Braun, S., & Brunet-Gouet, E. (2015). Characterizing an ERP correlate of intentions understanding using a sequential comic strips paradigm. *Social Neuroscience*, *10*, 391–407.

Wang, Y., Song, J., Guo, F., Zhang, Z., Yuan, S., & Cacioppo, S. (2016). Spatiotemporal brain dynamics of empathy for pain and happiness in friendship. *Frontiers in Behavioral Neuroscience*, *10*, 45.

Yu, H., Cai, Q., Shen, B., Gao, X., & Zhou, X. (2016, Decemeber 12). Neural substrates and social consequences of interpersonal gratitude: Intention matters. *Emotion*. PubMed PMID: 27936814.

Zigmond, A. S., & Snaith, R. P. (1983). The hospital anxiety and depression scale. *Acta Psychiatrica Scandinavica*, *67*, 361–370.